scientific reports

OPEN

Revolutionizing proton exchange membrane fuel cell modeling through hybrid aquila optimizer and arithmetic algorithm optimization

Manish Kumar Singla[1,2]✉, S. A. Muhammed Ali[1], Ramesh Kumar[3], Pradeep Jangir[4,5,6], Mohammad Khishe[7,8]✉, G. Gulothungan[9]✉ & Haitham A. Mahmoud[10]

Parameter identification in a Proton Exchange Membrane Fuel Cell (PEMFC) entails the application of optimization algorithms to ascertain the optimal unknown variables essential for crafting an accurate model that predicts fuel-cell performance. These parameters are typically not included in the manufacturer's datasheet and must be identified to ensure precise modeling and forecasting of fuel cell behavior. This paper introduces a recently developed hybrid algorithm (Aquila Optimizer Arithmetic Algorithm Optimization (AOAAO)) that enhances the AO and AAO algorithm's efficiency through a novel mutation strategy, aimed at determining seven unknown parameters of a PEMFC during the optimization process. These parameters function as decision variables, and the objective function aimed for minimization is the sum square error (SSE) between the predicted and actual measured cell voltages. AOAAO demonstrated superior performance across various metrics, achieving an SSE minimum in comparison to other compared algorithm. AOAAO's robustness was validated through extensive testing with six commercially available PEMFCs, including BCS 500 W-PEM, 500 W SR-12PEM, Nedstack PS6 PEM, H-12 PEM, HORIZON 500 W PEM, and a 250 W-stack, across twelve case studies derived from various operational conditions detailed in manufacturers' datasheets. For each datasheet, both Current–Voltage (I/V) and Power–Voltage (P/V) characteristics of the PEMFCs scenarios closely aligned with those observed in experimental data, affirming AOAAO's superior accuracy, robustness, and time efficiency for real-time fuel cell modeling. In terms of computational efficiency, AOAAO runtime is significantly faster than all compared algorithms, demonstrating an efficiency improvement of approximately 98%.

Keywords Parameter estimation, Proton exchange membrane fuel cell, Hybrid algorithm, Metaheuristic, Machine learning-inspired optimization

The finite nature and detrimental ecological consequences of fossil fuels necessitate a transition to environmentally benign energy alternatives[1]. Fuel cells, which convert chemical energy into electrical energy through electrochemical reactions, emerge as potential candidates for this transition[2]. As clean energy technologies, fuel

[1]Fuel Cell Institute, Universiti Kebangsaan Malaysia, Bangi 43600, Selangor, Malaysia. [2]Department of Biosciences, Saveetha School of Engineering, Saveetha Institute of Medical and Technical Sciences, Chennai 602 105, India. [3]Department of Interdisciplinary Courses in Engineering, Chitkara University Institute of Engineering & Technology, Chitkara University, Chandigarh, Punjab, India. [4]University Centre for Research and Development, Chandigarh University, Gharuan 140413, Mohali, India. [5]Department of CSE, Graphic Era Hill University, Graphic Era Deemed to be University, Dehradun 248002, Uttarakhand, India. [6]Applied Science Research Centre, Applied Science Private University, Amman 11937, Jordan. [7]Department of Electrical Engineering, Imam Khomeini Naval Science University of Nowshahr, Nowshahr, Iran. [8]Jadara University Research Center, Jadara University, Irbid, Jordan. [9]Department of Electronics and Communication Engineering, SRM Institute of Science and Technology, SRM Nagar, Kattankulathur, Chengalpattu 603203, Tamil Nadu, India. [10]Industrial Engineering Department, College of Engineering, King Saud University, Riyadh 11421, Saudi Arabia. ✉email: msingla0509@gmail.com; m_khishe@alumni.iust.ac.ir; g.gulothungan@gmail.com

cells distinguish themselves by their superior efficiency and capacity for emissions-free power generation[2,3]. In contrast to conventional power generators, fuel cells produce energy through the electrochemical reaction of hydrogen and oxygen[4,5]. This clean process substantially diminishes environmental impact, especially in terms of greenhouse gas emissions and air pollution[6]. Proton exchange membrane fuel cells (PEMFCs)[7], solid oxide fuel cells (SOFCs)[8], and molten carbonate fuel cells (MCFCs)[9] represent three distinct types of fuel cells that find applications in diverse domains. SOFCs, renowned for their fuel versatility and capacity to operate at elevated temperatures, are well-suited for stationary power generation[10]. Moreover, the modular design of fuel cells permits scalability, accommodating both compact, portable devices and large-scale power plants[11]. Consequently, fuel cells present a viable option for a variety of applications, including residential, commercial, and industrial energy supply[12].

PEMFCs have garnered recognition for their exceptional efficiency and minimal emissions[13]. This study centres on the precise modeling of PEMFCs with the aim of facilitating optimized design strategies that contribute to a cleaner and more sustainable future. In the midst of the global transition towards cleaner energy sources, PEMFCs play a pivotal role in reducing reliance on fossil fuels, mitigating pollution, and ensuring energy security[14]. Their increasing prominence in sectors such as transportation[15], distributed generation, and micro-grids underscores the importance of this research, which explores the domain of these clean energy options and future advancements in fuel cell technology[16]. The construction of accurate models for PEMFCs has become a focal point for researchers[17] who seek to establish reliable models using software programs that closely correlate with experimental results[18]. The significance of PEMFC modeling lies in its impact on analyses, particularly in micro-grids and smart grid applications[19].

Researchers use a mix of analytical, empirical, semi-empirical, and theoretical methods to model PEMFC performance[20–22]. Both traditional and advanced techniques, like metaheuristics, are used to extract PEMFC parameters[23]. Reference[24] dives deep into PEMFC parameter estimation, highlighting the challenges of nonlinear systems. The review emphasizes using empirical equations for design and introduces exciting new techniques like neural networks and bio-inspired algorithms. The drawbacks mentioned are GA's limited exploration and HSA's tendency to converge too quickly. Reference[25] introduces two new ways to solve a tough equation in PEMFC modeling and a hybrid optimization algorithm that beats existing methods for estimating PEMFC parameters. In[26], a semi-empirical PEMFC model is built using a new grey wolf optimization algorithm to capture real-world behavior. Reference[27] uses an empirical performance degradation model to assess aging factors and power loss by fitting parameters to polarization curves.

The drawbacks mentioned in this reference are: (1) the challenges associated with physical-based approaches for degradation modeling, (2) the reliance of data-driven approaches on experimental data that may lack understanding of degradation states, and (3) the difficulty in accurately predicting lifespan. The study presented in[28] evaluates six optimization techniques on PEMFC models, identifying performance disparities and highlighting the most accurate one, supported by MATLAB validations. The limitation in this reference is the high failure rate in the production of fuel cells, leading to high costs and low reliability. In[29], three metaheuristic optimization techniques are introduced to determine the parameters of PEMFCs, demonstrating that these methods solve the optimization problem with minimal differences in performance. Reference[30] proposes a semi-empirical approach that combines variational Bayes for parameter estimation and Sobol sensitivity analysis for PEMFC modeling, offering a high level of accuracy and reduced computational effort while quantifying parameter sensitivity and uncertainty under varying conditions. The limitations mentioned in this reference are: (1) the complexity of equations in mechanism models leading to long computation times, and (2) the data-driven models requiring a large amount of data and being time-consuming to build. The study in[31] examines the degradation prediction of a PEMFC stack through semi-empirical and data-driven models to forecast long-term stack performance degradation with improved accuracy. The drawbacks mentioned in this reference are: (1) the challenge of obtaining test data for the whole life cycle, and (2) the degradation processes of leaking current impacting the performance.

Reference[32] presents a novel semi-empirical model for PEMFC voltage estimation, optimizing parameters using the lightning search algorithm and validating the model under various conditions. The drawbacks mentioned in this reference are: (1) the semi empirical model for voltage prediction requiring correction through experimentation, (2) the parameters in the model varying with ambient conditions, affecting accuracy, and (3) semi empirical models lacking the complexity and accuracy of more sophisticated models. Reference[33] proposes a new optimization algorithm, Combined Owl Search Algorithm, for estimating optimal parameters in PEMFC fuel cell stacks, achieving lower errors compared to existing methods. A novel Dandelion Optimizer is proposed in[34] to accurately identify the parameters of the PEMFC model, addressing challenges associated with nonlinearity and the unknown parameters, with comparative analysis with existing optimization algorithms. The challenges with metaheuristic optimizers are getting stuck in local minima, and other optimizers are slow to converge. Accurately extracting PEMFC parameters remains a challenge due to limitations in modeling and validation.

This study aims to develop a robust and reliable PEMFC model that accurately represents experimental data. The model incorporates seven unknown design variables to capture the nonlinear I/V relationship. An objective function minimizes the SSE to determine optimal variable values. Various optimization algorithms, including Aquila Optimizer (AO)[36], Nuclear Reaction Optimization (NRO)[37], Kepler Optimization Algorithm (KOA)[38], Ring Clustering Algorithm (RCA)[39], Whale Optimization Algorithm (WOA)[40], Differential Evolution Algorithm (DE)[41], Particle Swarm Optimization (PSO)[42], Chimp Optimization Algorithm (ChOA)[43], and Arithmetic Optimization Algorithm (AOA)[44] algorithm, will be used to validate the model's robustness under different pressure and temperature conditions. The constant improvement of optimization techniques shows how important it is to optimize PEMFC performance. Researchers around the world are working to find the best optimization techniques and algorithms to reduce errors and boost efficiency. They're also focused on making algorithms simpler to reduce complexity and speed up calculations.

A novel hybrid optimization algorithm is introduced in the study, which synergizes the Aquila Optimizer and Arithmetic Optimization Algorithm with a chaotic mutation strategy and an energy inspired parameterization mechanism to improve search dynamics and convergence performance. This innovative integration of the components overcomes the limitations of existing optimization techniques, namely premature convergence and inefficiency in high dimensional or complex search spaces. The proposed method leverages chaotic maps to inject controlled randomness into the optimization process, and thus achieves a robust balance between exploration and exploitation, and avoids the risk of stagnation in local optima. The structured randomness greatly increases the diversity of the candidate solutions, and thereby improves the global search ability. The optimization method is shown to be very precise and adaptable in the domain of parameter estimation for Proton Exchange Membrane Fuel Cells (PEMFCs), a domain of nonlinear dynamics and multidimensional constraints. In contrast to conventional algorithms that frequently struggle to accurately represent the intricate electrochemical behaviors of PEMFC systems, the proposed approach obtains a very low Sum of Squared Errors over a wide range of stack configurations and operating conditions. This demonstrates its ability to produce optimal or near optimal solutions reliably under a variety of and difficult circumstances. This method is one of the most computationally efficient compared to state of the art methods. The proposed algorithm reduces runtime by up to 98% with or better than accuracy benchmarks, and is thus well suited for real time and large scale applications. This efficiency is further validated with rigorous statistical analyses, including multiple performance metrics, and comparative benchmarking against leading algorithms in the literature. The evaluations confirm not only the reliability of the method but also its ability to handle computational bottlenecks in optimization problems. Moreover, the hybrid approach is scalable and generalizable. The practical utility of the model in real world PEMFC applications is demonstrated by the fact that it can be adapted to different PEMFC configurations and operating parameters without requiring extensive modifications. This method is distinguished as a transformative solution in the field by the innovative combination of optimization strategies and its validated performance improvements. This work establishes a new benchmark in efficiency, robustness and accuracy for nonlinear system modeling and parameter estimation, filling persistent gaps in the literature, and paving the way for future developments in energy system optimization. The key contributions of this work are:

- Precise identification of PEMFC models based on minimizing the Sum of Squared Errors (SSE) between actual and estimated characteristics, using the AOAAO along with various compared algorithms.
- An in-depth analysis of the application of AOAAO variants including Aquila Optimizer (AO)[36], Nuclear Reaction Optimization (NRO)[37], Kepler Optimization Algorithm (KOA)[38], Ring Clustering Algorithm (RCA)[39], Whale Optimization Algorithm (WOA)[40], Differential Evolution Algorithm (DE)[41], Particle Swarm Optimization (PSO)[42], Chimp Optimization Algorithm (ChOA)[43], and Arithmetic Optimization Algorithm (AOA)[44] algorithm.
- Twelve different commercially available PEMFC stacks were analyzed, including BCS 500 W-PEM[45], 500 W SR-12PEM[26], Nedstak PS6 PEM[26], H-12 PEM[46], HORIZON 500 W PEM[46], and 250 W-stack[47].
- A full statistical evaluation was conducted to validate the consistency of the methods tested.
- The results achieved were benchmarked against findings from existing literature.

Literature review

The literature reviewed provides a comprehensive exploration of various advancements and methodologies in PEMFC research, such as shown in Table 1. Its extents various areas such as thermal management, optimization strategies, and geometrical design impacts on performance. Notable contributions include the development of intelligent algorithms for optimal temperature control in water-cooled PEMFC systems, innovative flow-field designs to enhance performance and hybrid optimization techniques for efficient parameter identification. Studies also delve into practical application, such as hydrogen storage solutions and sustainable energy production for fuel cell. These findings underscore the significance of integrating computational modeling, experimental validation, and cutting-edge algorithms to address operational challenges and optimize PEMFC efficiency and durability, making them critical for advancing sustainable energy systems.

PEMFC modeling

Proton Exchange Membrane Fuel Cells (PEMFCs) are complex systems that rely on electrochemical reactions to convert chemical energy into electrical energy. To better understand these intricate processes, researchers employ mathematical models and computer simulations. A simplified schematic of a PEMFC is shown in Fig. 1.

The distribution of chemical species, such as hydrogen, oxygen and water, within the fuel cell has a significant impact on the performance of a PEMFC. The distributions of these parameters affect reaction rates, mass transport, and thermal management. The polarization and power density curves give some insight into overall performance, but do not characterize the localized variations and complexities arising from species distributions. The model presented here aims to estimate parameters and optimize performance based on global characteristics, such as voltage and current density relationships. However, it is not granular enough to understand internal processes and localized performance bottlenecks without the ability to predict the spatial and temporal distributions of species. The model could then account for gradients in concentration, temperature, and other critical parameters by incorporating the prediction of species distributions. This enhancement would allow greater understanding of water flooding, dry out, and catalyst utilization, all of which directly influence PEMFC efficiency and durability. In addition, predictive capability of this type would be extremely useful for designing advanced control strategies and improving system reliability under varying operating conditions. This capability could be developed by coupling the current model with detailed multi-physics simulations, or by

S. no.	Work	Related area	Findings	Methodology	Relevance	Citation
1	Modelling and temperature control of a water-cooled PEMFC system using intelligent algorithms	Thermal management in water-cooled PEMFC systems	Developed intelligent algorithms for maintaining optimal temperature	Computational modelling combined with machine learning algorithms	Emphasizes the importance of thermal control for sustained PEMFC performance and durability	48
2	Comparative Sustainability Analysis of PEMFC Designs	Flow-field designs in PEMFCs	Performance between serpentine and straight-channel designs	Experimental comparisons and metrics	Optimizing PEMFC performance and sustainability	49
3	Hybrid Optimization Techniques in Fuel Cell Research	Advanced optimization techniques	Advancements in hybrid algorithms for fuel cell research	Literature review and comparative analysis	Provides optimization strategies for fuel cell systems	50
4	Improved Computational with Thermodynamic Analysis of Hydrogen Generation	Algorithmic advancements for PEMFC	Hybrid optimization algorithms for parameter identification	Hybridization of algorithms such as AO and AAO	Enhances the accuracy and efficiency of PEMFC	51
5	Advanced Hydrogen Generation with deep learning and statistical methods	Hydrogen performance of fuel properties	Explores how different fuel characteristics	Experimental analysis and fuel characterization	Expands fuel properties affect Hydrogen durability and performance	52
6	Modelling and temperature control of a water-cooled PEMFC system	Thermal management in PEMFCs	Developed algorithms for optimal PEMFC operating temperatures	Computational modelling with control algorithms	Thermal management for long-term PEMFC performance	48
7	Integration of Novel P PEM Fuel Cells Systems in Practical Applications	Practical applications of PEMFC technology	challenges and solutions for automotive and power systems	Case studies and system-level analysis	Demonstrates of Exploring the Sustainability of Serpentine Flow-Field Fuel Cell	53
8	Advanced Research on Fuel Cell-based Hybrid Electric Vehicles	Broad advancements in Fuel Cell research	Explores techniques and applications for Fuel Cell	Experimental, modelling, developments	Provides diverse perspectives and updates in Fuel Cell	54
9	Research on the performance characteristics of hydrogen for PEMFC vehicles	Hydrogen circulation in PEMFC vehicles	Performance metrics for hydrogen pumps; impact	Experimental studies and performance evaluation	Provides insights into the practical challenges and advancements	55
10	Performance Optimization of PEMFCs	Optimization strategies	Explores non-traditional operational parameters	Theoretical modelling supported by experimental validation	Suggests innovative approaches for PEMFC systems	56
11	Innovative Cooling Techniques for Enhanced PEMFC Longevity	Cooling and thermal management in PEMFC systems	Investigates advanced cooling techniques to ensure long-term durability and performance	Computational fluid dynamics (CFD) and thermal modeling	Provides new strategies for overcoming thermal challenges in PEMFC applications	57
12	Experimental and modelling for multi-channel PEMFC	Geometrical design impacts on PEMFC performance	Analyses single- and multi-channel PEMFC designs and performance	Experimental and computational modelling	Demonstrates geometrical designs affect PEMFC efficiency and durability	58
13	Investigating Hydrogen Storage and Circulation for PEMFCs	Hydrogen storage and impact on PEMFCs	Focused on hydrogen storage solutions efficiency	Experimental designs and modelling approaches	hydrogen management for optimized PEMFC operations	59
14	Study of parameters of proton exchange membrane	Operating parameters of PEMFCs	Correlations between operating conditions and cell efficiency	Experimental testing with varying operational scenarios	Demonstrates for enhancing PEMFC operational efficiency.	60
15	Challenges of PEMFC Parameter Identification and Algorithm Justification	Algorithmic challenges in PEMFC modelling	Traditional algorithms and reviews advance in hybrid algorithms	Literature review with specific focus on AO and AAO hybridization	Hybrid algorithms in addressing complex PEMFC parameter challenges	61
16	Work on HT-PEMFC testing	HT-PEMFC testing and development	Developed an HT-PEMFC test cell and testing station	Engineering design and performance testing	Provides testing and improving high-temperature PEMFCs	62
17	Demonstrates PEMFC stack performance	PEMFC stack simulation	PEMFC stack performance for portable power generation	Computational modelling and simulation approaches	Stack viability for compact and portable power solutions	63
18	Work on hydrogen as a energy source for PEMFC	Bio-hydrogen for PEMFC	Reviews for bio-hydrogen production	Literature review on bio-hydrogen processes	Highlights bio-hydrogen as a promising renewable energy source	64
19	Optimisation of water and reactant management in PEMFCs	Flow field design in PEMFCs	Examines the affects water management and reactant distribution	Comparative analysis of flow field geometries	Optimizes water and reactant management	65
20	An Innovative Approach on the Performance of PEMFC	Diffusion rate of reactants in PEMFCs	Identified factors rate and their effects on cell performance	Innovative predictive modelling to analyse diffusion impacts	Reactant diffusion in optimizing fuel cell performance.	66

Table 1. Literature reviewed provides a comprehensive exploration of various advancements and methodologies.

adding additional equations to represent mass transport and reaction kinetics. This would obviously increase the computational complexity, but create a much more robust, and thus full, tool for PEMFC analysis. Overcoming this limitation would elevate the model from a performance estimation tool to a full predictive framework, similar in spirit to what is required for modern PEMFC design and optimization.

PEMFCs, however, face several challenges that limit their performance. These challenges are primarily associated with voltage losses, which can be categorized into three types.

Activation losses

These occur at low current densities, particularly during start-up, when the electrochemical reactions are sluggish. This results in a rapid voltage drop.

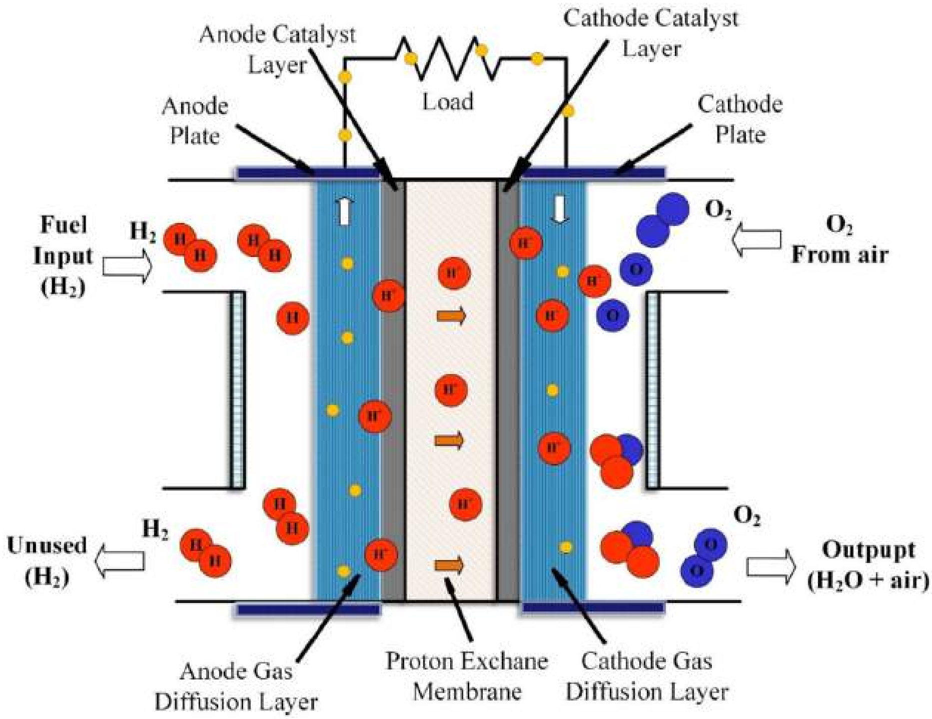

Fig. 1. Schematic of PEMFC.

Ohmic losses

As the current density increases, resistance to the flow of ions and electrons within the fuel cell grows, leading to a gradual decrease in voltage.

Concentration losses

At high current densities, reactant concentrations can diminish due to mass transport limitations, such as water build-up. This can significantly reduce voltage output.

To enhance the efficiency and performance of PEMFCs, researchers are actively working on strategies to mitigate these voltage losses. This includes developing advanced catalysts, optimizing flow field designs, and improving reactant gas management techniques.

So, Eq. 1 can be used to show the PEMFC terminal voltage:

$$V_{FC} = E_{Nernest} - v_{act} - v_{ohm} - v_{conc}. \tag{1}$$

For temperatures below 100 °C, the reversible open-circuit voltage, E_{Nernst}, can be calculated using Eq. 2.

$$E_{Nernest} = 1.229 - 8.5 \times 10^{-4} \times (T_{FC} - 298.15) + 4.3085 \times 10^{-5} \times T_{FC} \times \ln\left(P_{H_2}\sqrt{P_{O_2}}\right) \tag{2}$$

where T_{FC} is the cell temperature in Kelvin, and P_{H2} and P_{O2} are the partial pressures of hydrogen and oxygen, respectively.

Equation 3 approximates the activation voltage loss (v_{act}).

$$v_{act} = -\left[\xi_1 + (\xi_2 \times T_{FC}) + (\xi_3 \times T_{FC} \times \ln(C_{O_2})) + (\xi_4 \times T_{FC} \times \ln(I_{fc}))\right] \tag{3}$$

I_{FC} is the fuel cell current, and ξ_1 to ξ_4 are some numbers. C_{O2} and C_{H2} are the oxygen concentration in mol/cm^3, and we can calculate them using Eqs. 4 and 5.

$$C_{O_2} = \frac{P_{O_2}}{5.08 \times 10^6} \times \exp^{\left(\frac{498}{T_{FC}}\right)} \tag{4}$$

$$C_{H_2} = \frac{P_{H_2}}{1.09 \times 10^6} \times \exp^{\left(\frac{-77}{T_{FC}}\right)} \tag{5}$$

The ohmic voltage loss, v_{ohm}, is calculated using the fuel cell's resistance and is defined by Eq. 6.

$$v_{ohm} = I_{FC} \times (R_m + R_c) \tag{6}$$

Here, R_m and R_c represent the membrane and contact resistances, respectively. Equations 7 and 8 can be used to calculate R_m.

$$R_m = \frac{\rho_m \times l}{M_A} \tag{7}$$

$$\rho_m = \frac{181.6 \times \left[1 + 0.03 \times J + 0.062 \times J^{2.5} \times (T_{FC}/303)^2\right]}{[\lambda - 0.634 - 3 \times J] \times \exp^{\left(4.18 \times (T_{FC} - 303)/T_{fc}\right)}} \tag{8}$$

Here, ρ_m, l, A_m, J, *and* λ represent the membrane resistivity (Ω.cm), thickness (cm), active area (cm²), real current density (A/cm²), and water content, respectively. Equation 9 can be used to estimate v_{conc}.

$$v_{conc} = -\beta \times \ln(1 - J/J\text{max}) \tag{9}$$

Here, β is the maximum current density (A/cm²) and J_{max} is a constant coefficient.

PEMFC stacks are made up of multiple cells (N_{cells}). The stack voltage (V_{stack}) is calculated using Eq. 10.

$$V_{stack} = N_{cells} \times V_{FC} = N_{cells} \times (E_{Nernest} - v_{act} - v_{ohm} - v_{conc}) \tag{10}$$

This equation assumes that all cells behave identically and ignores the connecting resistors.

To accurately describe the mathematical model, seven unknown parameters (ξ_1 to ξ_4, λ, and β) must be identified. Mann's model[35] utilizes an iterative approach to estimate these parameters. Precise parameter estimation is essential for any mathematical model. It involves integrating experimental data, computer simulations, and optimization techniques to minimize the difference between the model's predictions and actual observations.

Significance of the PEMFC model

- *Performance prediction* To simulate and predict the performance of PEMFCs under various operating conditions (temperature, pressure, humidity, etc.). This allows researchers to identify optimal design parameters, such as stack configuration, flow channel geometries, and operating conditions, leading to enhanced efficiency and power output.
- *Durability analysis* By analyzing complex degradation mechanisms, it can help in predict the lifespan of PEMFCs and identify critical factors that contribute to performance degradation. This knowledge can guide the development of more durable and long-lasting fuel cells.
- *Advanced simulations* The model can be used to develop and refine sophisticated mathematical models of PEMFC behavior, capturing complex phenomena like multiphase flow, electrochemical reactions, and transport processes. These models can provide deeper insights into fuel cell operation and enable more accurate predictions of performance.
- *Machine learning integration* Model can be integrated with machine learning algorithms to develop predictive models that can accurately estimate fuel cell performance based on various input parameters. This can accelerate the optimization process and enable more efficient design of new fuel cell systems.

Problem formulation

This paper presents a method to improve the accuracy of a PEMFC model by aligning its predicted voltage with real-world measurements. The model employs mathematical equations to forecast voltage output at any given current. To enhance its precision, a specialized algorithm is utilized. The effectiveness of this approach is assessed by comparing predicted and measured voltage values using the Sum of Squared Error (SSE), as defined in Eq. 11.

$$\text{SSE} = \text{ MIN}\left(\text{F} = \sum{}_{\text{i}=1}^{\text{N}}(\text{V}_{\text{actual}} - \text{V}_{\text{i}})^2\right) \tag{11}$$

Here, actual experiment voltage is denoted by V_{actual}, computed model voltage is denoted by V_{i}, and N is the number of data points.

Algorithm

Aquila optimizer

The aquila optimizer (AO)[36] employs four predation strategies to simulate the behavior of individuals in a swarm as they catch prey.

Strategy first

Soaring high above the landscape in search of prey, the Aquila eagle surveys the hunting ground from a lofty vantage point. Upon identifying a prey, it dives vertically toward the prey. This behavior is expressed mathematically as:

$$X(t+1) = X_{\text{best}}(t) \times \ (1 - t/T) + (X_M(t) - X_{\text{best}}(t) \times \ \text{rand}) \tag{12}$$

Here, $X(t+1)$ denotes the positions of individuals at the $t+1$ iteration, $X_{\text{best}}(t)$ represents the global best position at the t-th iteration, t and T denote the current iteration and the maximum allowed iteration number, respectively. $X_M(t)$ refers to the mean position of individuals at the current iteration, and rand is a random number generated from a Gaussian distribution within the interval $[0,1]$.

Strategy second

The Aquila eagle employs a tactical maneuver known as contour flight, which involves transitioning from high-altitude soaring to a hovering position directly above its prey. This strategic positioning sets the stage for a swift and decisive predatory strike. The update of positions is governed by the equation:

$$X(t+1) = X_{\mathrm{best}}(t) \times \mathrm{LF}(D) + X_R(t) + (y - x) \times \mathrm{rand} \tag{13}$$

Here, $X_R(t)$ denotes the random position of Aquila, and D signifies the size of the dimension. The term LF represents the Levy flight function, while y and x describe the shape of the search. These can be calculated using:

$$\begin{cases} x = (r_1 + 0.00565 \times D_1) \times \sin(-\omega \times D_1 + (3 \times \pi)/2) \\ y = (r_1 + 0.00565 \times D_1) \times \cos(-\omega \times D_1 + (3^2 \times \pi)/2) \end{cases} \tag{14}$$

The Levy flight function, denoted as $\mathrm{LF}(x)$, is defined as:

$$\mathrm{LF}(x) = 0.01 \times \frac{\mu \times \sigma}{|\nu|^{1/\beta}} \text{ where } \sigma = \left(\frac{\Gamma(1+\beta) \times \sin(\pi\beta/2)}{\Gamma((1+\beta)/2) \times \beta \times 2^{((\beta-1)/2)}} \right)^{1/\beta} \tag{15}$$

Here, r_1 refers to the number of search cycles ranging from 1 to 20, D_1 is a random integer from 1 to the dimension D, and ω is a constant set to 0.005.

Strategy third

The Aquila eagle adopts a low-altitude flight strategy to approach and target its prey. By carefully identifying and locating the prey, the eagle descends for an initial predatory strike. The equation governing this behavior is:

$$X(t+1) = (X_{\mathrm{best}}(t) - X_M(t)) \times \alpha - \mathrm{rand} + ((UB - LB) \times \mathrm{rand} + LB) \times \delta \tag{16}$$

In this equation, α and δ are parameters for adjustment during the development process and are fixed at 0.1. The terms UB and LB denote the upper and lower bounds of the search space, respectively.

Strategy fourth

The Aquila eagle demonstrates remarkable adaptability by pursuing its prey onto land. It meticulously tracks the prey's escape route, relentlessly following and attacking until the hunt is successful. The behavior is mathematically formulated as:

$$X(t+1) = QF \times X_{\mathrm{best}}(t) - (G_1 \times X(t) \times \mathrm{rand}) - G_2 \times \mathrm{LF}(D) + \mathrm{rand} \times G_1 \tag{17}$$

The quality function (QF) of the search strategy is described as:

$$QF(t) = t^{(2 \times \mathrm{rand} - 1)/((1-T)^2)} \tag{18}$$

The parameters G_1 and G_2 are defined as:

$$\begin{cases} G_1 = 2 \times \mathrm{rand} - 1 \\ G_2 = 2 \times (1 - t/T) \end{cases} \tag{19}$$

Here, QF is a measure of the search strategy's quality, G_1 represents the random motion parameter during Aquila's prey-tracking process, taking values in the range $[-1,1]$, and G_2 describes the flight slope during prey tracking, decreasing linearly to 0.

Arithmetic optimization algorithm

The Arithmetic Optimization Algorithm (AOA) leverages four essential arithmetic operators to efficiently balance exploration and exploitation during the optimization process.

Exploration phase

During the exploration phase, the division and multiplication operators are utilized due to their ability to generate highly distributed values. This characteristic prevents easy convergence to the target, making these operators ideal for the search phase. The position update during this phase can be expressed as:

$$X(t+1) = \begin{cases} X_{best}(t) \div (MOP + \in) \times ((UB - LB) \times \mu + LB), & r_2 < 0.5 \\ X_{best}(t) \times MOP \times ((UB - LB) \times \mu + LB), & otherwise \end{cases} \tag{20}$$

Here, $\in$ represents a small integer, and μ is a control parameter fixed at 0.5 during the search process. The Math Optimizer Probability (MOP) serves as a coefficient. α is a sensitive coefficient, set at 5, to define development accuracy. The Math Optimizer Accelerated (MOA) is employed to select the search phase. The parameters

Max and Min represent the maximum and minimum values of the acceleration function, respectively. These values are calculated using the equations:

$$\begin{aligned} MOP\,(t) &= 1 - t^{1/\alpha}\,/T^{1/\alpha}\,, \\ MOA\,(t) &= Min + t \times\, ((Max - Min)/T). \end{aligned} \tag{21}$$

Exploitation phase
In this phase, subtraction and addition operators are used due to their ability to produce high-density results. These operators are characterized by low dispersion, enabling them to approach the target effectively. These characteristics align with the requirements of the exploitation phase. The position update for this phase is expressed as:

$$X(t+1) = \begin{cases} X_{\text{best}}\,(t) - MOP \times\, ((UB - LB) \times\, \mu\, + LB), & r_3 < 0.5 \\ X_{\text{best}}\,(t) + MOP \times\, ((UB - LB) \times\, \mu\, + LB), & \text{otherwise} \end{cases} \tag{22}$$

The defects and improved algorithm

During the exploration phase, AOA individuals exhibit rapid flight and predation behavior within the search space. The direct integration of the global best position into the position update mechanism accelerates convergence and enhances search capabilities. However, this approach frequently results in premature convergence, trapping individuals in local optima. Experimental findings suggest that the division and multiplication operators employed during the exploration phase in AOA exhibit relatively slow convergence rates. Furthermore, the population diversity and search agent volatility are inadequate, and the transition mechanism between exploration and exploitation is suboptimal. To mitigate these shortcomings, refinements are essential.

Hybridization of AO with AAO algorithm
An analysis of Eqs. (12), (13), (20), and (22) reveals that AOA individuals engage in more random exploration during the initial phase compared to AO swarms. Conversely, during the exploitation phase, as defined by Eqs. (16), (17), (20), and (22), AOA individuals demonstrate suboptimal performance relative to AO swarms.

While both algorithms exhibit strong optimization capabilities, AO swarms exhibit a less effective exploitation phase, whereas AOA swarms demonstrate a weaker exploration phase. As a result, a hybrid approach that merges the exploration phase of AO swarms with the exploitation phase of AOA swarms could potentially lead to superior performance.

Energy parameter balancing exploration and exploitation ratio
To synergize the exploration process of AO swarms with the exploitation phase of AOA swarms, an additional parameter is introduced to modulate individual behavior within the combined algorithm. While random numbers could be employed, the energy parameter, inspired by the successful initial phases of the Harris Hawk Optimization (HHO) algorithm, is chosen instead. The energy parameter is mathematically represented as:

$$E = 2E_0(1 - t/T) \tag{23}$$

Here, E_0 denotes the initial energy of the prey, which is randomly selected from the range $[-1{,}1]$. In accordance with the HHO algorithm, when $|E| \geq\, 1$, the Harris Hawk begins searching for the prey's position. Conversely, when $|E| < 1$, the Harris Hawk proceeds to capture the prey.

Piecewise linear map
Chaos theory is considered a suitable alternative to randomness in optimization processes. To enhance the algorithm, chaotic mappings are incorporated. Specifically, the piecewise linear map is employed, which is mathematically defined as:

$$x(n+1) = \begin{cases} x_n/(1-\lambda\,), & 0 < x_n < 1 - \lambda \\ (x_n - (1 - \lambda\,))\,/\lambda\,, & 1 - \lambda\, < x_n < 1 \end{cases} \tag{24}$$

Using this chaotic mapping, an energy parameter that incorporates chaos is introduced into the hybrid algorithm. The enhanced energy parameter is expressed as:

$$E = 2E_0(1 - t/T) + \omega_{\,\max} - (\omega_{\,\max} - \omega_{\,\min}) \cdot \tfrac{t}{T} \cdot x_n \tag{25}$$

In this expression, λ is assigned a value of 0.6, while $\omega_{\,\max}$ and $\omega_{\,\min}$ are set to 0.9 and 0.5, respectively. The variable x_n represents the current solution. The improved energy parameter increases the system's volatility, allowing more individuals to remain in the exploration phase toward the end of the iteration process.

The proposed AOAAO algorithm
The hybridization of AOA and AO, enabled by the piecewise linear map, is proposed and abbreviated as AOAAO. The individuals in AOAAO swarms execute a more complex set of choices while updating their positions. The algorithm involves additional parameters; however, the overall time complexity remains nearly unaffected and is expressed as $O(T \cdot\, N \cdot\, D + N)$.

The AOAAO algorithm is a hybrid optimization technique that combines the strengths of AOA and AO algorithms. It utilizes a piecewise linear map to introduce chaotic behavior, enhancing exploration capabilities.

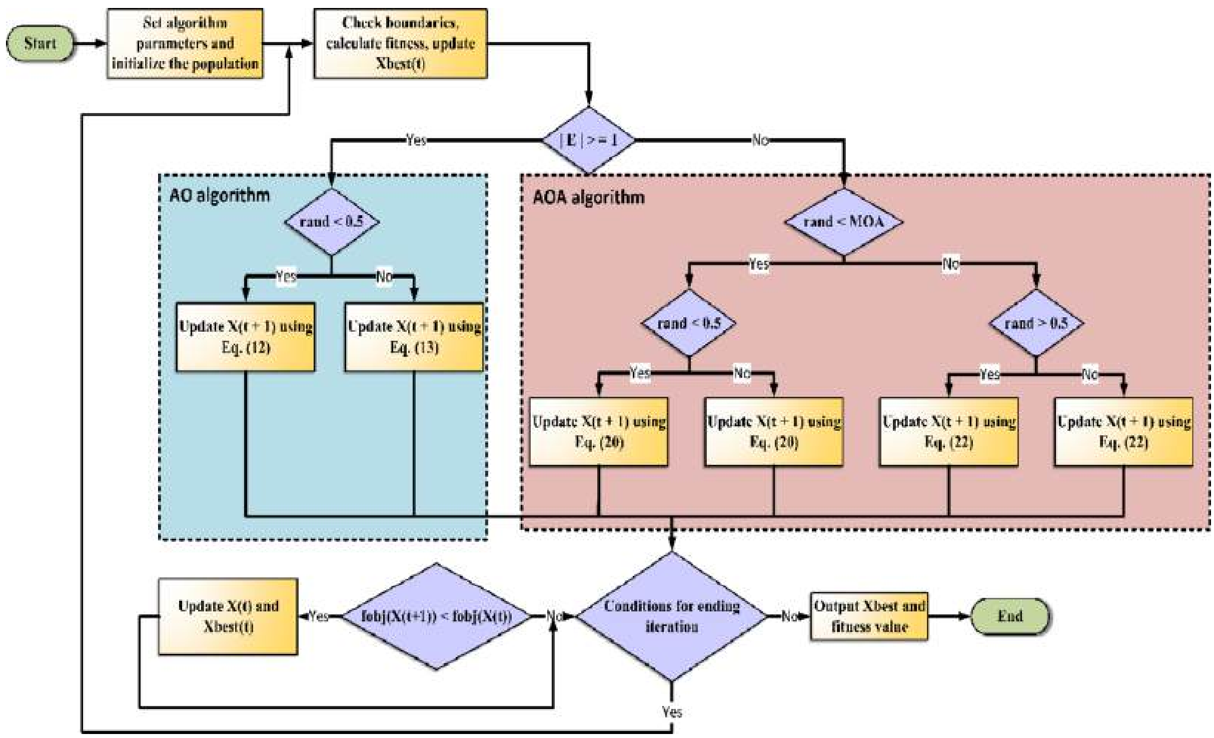

Fig. 2. Flowchart of hybrid proposed algorithm.

S.NO	Sheet 1	SHEET 2	SHEET 3	SHEET 4	SHEET 5	SHEET 6	SHEET 7	SHEET 8	SHEET 9	SHEET 10	SHEET 11	SHEET 12
PEMFC type	BCS 500 W	NetStack PS6	SR-12	H-12-1	Ballard Mark V	STD – 1	Horizon	STD – 2	STD – 3	STD – 4	H-12-2	H-12-3
Power (W)	500	6000	500	12	5000	250	500	250	250	250	12	13
Ncells (no)	32	65	48	13	35	24	36	24	24	24	13	13
A(cm^2)	64	240	62.5	8.1	232	27	52	27	27	27	8.1	8.1
l(um)	178	178	25	25	178	127	25	127	127	127	25	25
T(K)	333	343	323	323	343	343	338	343	343	343	302	312
Jmax(mA/cm^2)	469	1125	672	246.9	1500	860	446	860	860	860	246.9	246.9
PH_2(bar)	1.0	1.0	1.47628	0.4935	1.0	1.0	0.55	1.5	2.5	2.5	0.4	0.5
PO_2(bar)	0.2095	1.0	0.2095	1.0	1.0	1.0	1.0	1.5	3.0	3.0	1.0	1.0

Table 2. Twelves PEMFCs manufacturer sheets.

By integrating AOA's exploration and AO's exploitation, along with the influence of energy parameters, AOAAO aims to achieve a more robust and efficient search process while maintaining a balance between exploring the entire search space and exploiting promising regions, ultimately leading to improved solutions for various optimization problems.

The process for position updates, guided by the hybrid AOAAO algorithm, ensures improved exploration and exploitation balance through the combined use of energy parameters and chaotic mapping. The Fig. 2 represents the flowchart of the proposed hybrid algorithm and Algorithm 1 shows the pseudocode of the proposed algorithm.

Results and discussion

This work focuses on comparing the AOAAO algorithm to several compared variants, including Nuclear Reaction Optimization (NRO)[37], Kepler Optimization Algorithm (KOA)[38], Ring Clustering Algorithm (RCA)[39], Whale Optimization Algorithm (WOA)[40], Differential Evolution Algorithm (DE)[41], Particle Swarm Optimization (PSO)[42], Chimp Optimization Algorithm (ChOA)[43], Arithmetic Optimization Algorithm (AOA)[44], and Aquila Optimizer (AO)[36] to assess their performance in PEMFC modeling. All algorithms were configured with their recommended settings to estimate parameters for various PEMFC fuel cells (BCS 500 W-PEM, 500 W SR-12PEM, Nedstak PS6 PEM, H-12 PEM, HORIZON 500 W PEM, and 250 W-stack) listed in Table 2. Experiments were conducted on MATLAB 2022 A on a Windows Server 2022 PC with an i7-11700k@3.6 GHz CPU, using 700 maximum iterations, 30 runs, and a population size of 40. Table 3 shows the upper and lower bound of the sheet and Table 4 shows the parameter settings of the algorithm.

Parameter	Lower bound	Upper bound
ξ_1	− 1.1997	− 0.8532
ξ_2	1×10^{-3}	5×10^{-3}
ξ_3	3.6×10^{-5}	9.8×10^{-5}
ξ_4	-26×10^{-5}	-9.54×10^{-5}
λ	13	24
$R_c(\Omega)$	1×10^{-4}	8×10^{-4}
β (V)	0.0136	0.5

Table 3. Boundaries of model parameters.

Algorithm	Parameter setting
NRO	$P_{\mathrm{Fi}} = \mathrm{rand},\ P_{\mathrm{B}} = \mathrm{rand},\ \mathrm{and\ Freq} = 0.05$
KOA	$T_{\mathrm{c}} = 3,\ M_{\mathrm{o}} = 0.1,\ \lambda = 15$
WOA	$b = 1,\ a_1 =\in [0,2],\ a_2 =\in [-2,-1]$
DE	F = 0.5, CR = 0.9
PSO	W = 1, Wp = 0.99, $C_1 = 1.5$, $C_2 = 2.0$
ChoA	A = 0.5, b = 0.2, $Z_1 = 0.7$, $Z_2 = 4$, $Z_3 = 0.6$, $P = 0.4$, U = 1.07
AOA	$MOP_{max} = 1$, $MOP_{min} = 0.2$, $\alpha = 5$, $\mu = 0.499$
AO	A = 0.1, $\beta = 1.5$, Delta = 0.1

Table 4. Parameters settings.

Pseudo code of the hybrid AOAAO algorithm.

```
Set population size N
Set the maximum number of iterations T
Set dimension D
Initialize the positions of Individuals X_i (i = 1,2, ..., N)

While t ≤ T
  Update the MOA and MOP using Eq. (21)
  Update x, y using Eq. (14)

For i = 1: N
    If |E| ≥ 1
      If rand < 0.5
        Update the position of X(t + 1) using Eq. (12)
      Else
        Update the position of X(t + 1) using Eq. (13)
      End if
    Else
      If rand < MOA
        If rand > 0.5
          Update the position of X(t + 1) using Eq. (20)
        Else
          Update the position of X(t + 1) using Eq. (20)
        End if
      Else
        If rand > 0.5
          Update the position of X(t + 1) using Eq. (22)
        Else
          Update the position of X(t + 1) using Eq. (11)
        End if
      End if
    End if
  End For

For i = 1: N
    Check if the position goes out of the search space boundary and bring it back
    Calculate the fitness of X(t)
    Update X_best(t)
  End For

t = t + 1
End While

Return X_best(t)
```

Algorithm 1. Pseudo-code of hybrid proposed algorithm.

SHEET 1: BCS 500 W parameter optimization

AOAAO outperforms other differential evolution algorithms in terms of stability, precision, and computational efficiency. A detailed analysis of the metrics in Table 5 reveals that AOAAO consistently records the lowest minimum, maximum, mean, and standard deviation values. For example, AOAAO's minimum value of 0.025493 is lower than AOA, AO and remaining compared algorithms indicating superior predictability and minimal error margins. Additionally, AOAAO's maximum value of 0.025625 is lower than AOA and AO. The standard deviation for AOAAO is almost negligible at 5.92E-05, reflecting less variability compared to AOA and AO. In terms of computational efficiency, AOAAO runtime (RT) of 0.192218 s is significantly faster than all compared algorithms, demonstrating an efficiency improvement of approximately 98%. Furthermore, AOAAO highest Friedman ranking (FR) of 1.2, compared to other algorithms, confirms its superior performance across all evaluation metrics. Table 6 provides a detailed comparison of experimental and calculated values, while Fig. 3 illustrates the I/V and P/V curves, error curves, convergence curves, and box plots, visually demonstrating AOAAO exceptional performance and its significant advantage over other algorithms.

SHEET 2: NetStack PS6 parameter optimization

AOAAO outperforms other differential evolution algorithms in terms of stability, precision, and computational efficiency. A detailed analysis of the metrics in Table 7 reveals that AOAAO consistently records the lowest minimum, maximum, mean, and standard deviation values. For example, AOAAO's minimum value of 0.275211

Algorithm	NRO	KOA	RCA	WOA	DE	PSO	ChOA	AOA	AO	AOAAO
ξ_1	− 0.98401	− 1.17707	− 0.8532	− 0.87108	− 1.15643	− 0.95535	− 1.12095	− 1.1723	− 0.96462	− 0.8532
ξ_2	0.00301	0.003251	0.003079	0.002331	0.00337	0.002577	0.003231	0.003733	0.002851	0.00218
ξ_3	6.45E-05	4.23E-05	9.39E-05	4.23E-05	5.4E-05	4.18E-05	5.19E-05	7.43E-05	5.85E-05	0.000036
ξ_4	− 0.00018	− 0.00019	− 0.00019	− 0.00019	− 0.00019	− 0.00019	− 0.00019	− 0.00019	− 0.00018	− 0.00019
λ	20.68135	20.16795	23	21.58818	20.88868	21.55567	20.94073	20.88438	16.61556	20.87724
R_c	0.000751	0.00012	0.000282	0.000217	0.000105	0.000157	0.000106	0.0001	0.000323	0.0001
B	0.0136	0.015599	0.016265	0.015927	0.016108	0.015973	0.016076	0.016131	0.013744	0.016126
Min.	0.055008	0.026139	0.025656	0.025942	0.025505	0.02618	0.025546	0.025493	0.073793	0.025493
Max.	0.19249	0.031945	0.085535	0.033361	0.025796	0.049968	0.026142	0.025646	0.140884	0.025625
Mean	0.113376	0.028178	0.046848	0.029216	0.025631	0.033557	0.025789	0.025532	0.098178	0.025519
Std.	0.053443	0.002446	0.022626	0.003695	0.000119	0.009998	0.000233	6.39E-05	0.028865	5.92E-05
RT	3.606325	5.002351	3.226045	3.075384	6.38224	3.657268	3.637633	4.144864	6.463723	0.192218
FR	9.4	5.8	7.6	6.2	3.2	6.6	3.8	2	9.2	1.2

Table 5. Optimized parameters and optimal function value for sheet 1.

S_NO	Icell	Vcell	Vest	Pref	Pest	AE	RE %	MBE
1	0.6	29	28.99722	17.4	17.39833	0.002777	0.009575	4.28E-07
2	2.1	26.31	26.30594	55.251	55.24247	0.004063	0.015443	9.17E-07
3	3.58	25.09	25.09356	89.8222	89.83493	0.003555	0.01417	7.02E-07
4	5.08	24.25	24.25462	123.19	123.2135	0.00462	0.019053	1.19E-06
5	7.17	23.37	23.37542	167.5629	167.6017	0.005416	0.023175	1.63E-06
6	9.55	22.57	22.58461	215.5435	215.6831	0.014615	0.064754	1.19E-05
7	11.35	22.06	22.07133	250.381	250.5096	0.011327	0.051348	7.13E-06
8	12.54	21.75	21.75846	272.745	272.8511	0.008463	0.038913	3.98E-06
9	13.73	21.45	21.46126	294.5085	294.6631	0.011263	0.052506	7.05E-06
10	15.73	21.09	20.98774	331.7457	330.1372	0.102258	0.484867	0.000581
11	17.02	20.68	20.69451	351.9736	352.2206	0.014509	0.070162	1.17E-05
12	19.11	20.22	20.23099	386.4042	386.6141	0.010986	0.054332	6.71E-06
13	21.2	19.76	19.77094	418.912	419.144	0.010943	0.055381	6.65E-06
14	23	19.36	19.36602	445.28	445.4186	0.006025	0.03112	2.02E-06
15	25.08	18.86	18.86647	473.0088	473.171	0.006466	0.034286	2.32E-06
16	27.17	18.27	18.27472	496.3959	496.5242	0.004721	0.025838	1.24E-06
17	28.06	17.95	17.95331	503.677	503.7699	0.003311	0.018444	6.09E-07
18	29.26	17.3	17.29288	506.198	505.9896	0.007123	0.041174	2.82E-06
						0.012913	0.061363	3.61E-05

Table 6. Performance metrics of AOAAO algorithm for sheet 1.

is lower than AOA, AO and remaining compared algorithms indicating superior predictability and minimal error margins. Additionally, AOAAO's maximum value of 0.275211 is lower than AOA and AO. The standard deviation for AOAAO is almost negligible at 5.84E-16, reflecting less variability compared to AOA and AO. In terms of computational efficiency, AOAAO runtime of 0.193296 s is significantly faster than all compared algorithms, demonstrating an efficiency improvement of approximately 98%. Furthermore, AOAAO highest Friedman ranking of 1, compared to other algorithms, confirms its superior performance across all evaluation metrics. Table 8 provides a detailed comparison of experimental and calculated values, while Fig. 4 illustrates the I/V and P/V curves, error curves, convergence curves, and box plots, visually demonstrating AOAAO exceptional performance and its significant advantage over other algorithms.

SHEET 3: SR-12 parameter optimization

AOAAO outperforms other differential evolution algorithms in terms of stability, precision, and computational efficiency. A detailed analysis of the metrics in Table 9 reveals that AOAAO consistently records the lowest minimum, maximum, mean, and standard deviation values. For example, AOAAO's minimum value of 0.242284 is lower than AOA, AO and remaining compared algorithms indicating superior predictability and minimal error margins. Additionally, AOAAO's maximum value of 0.242927 is lower than AOA and AO. The standard deviation for AOAAO is almost negligible at 0.000288, reflecting less variability compared to AOA and AO. In terms of computational efficiency, AOAAO runtime of 0.138754 s is significantly faster than all compared algorithms, demonstrating an efficiency improvement of approximately 98%. Furthermore, AOAAO highest

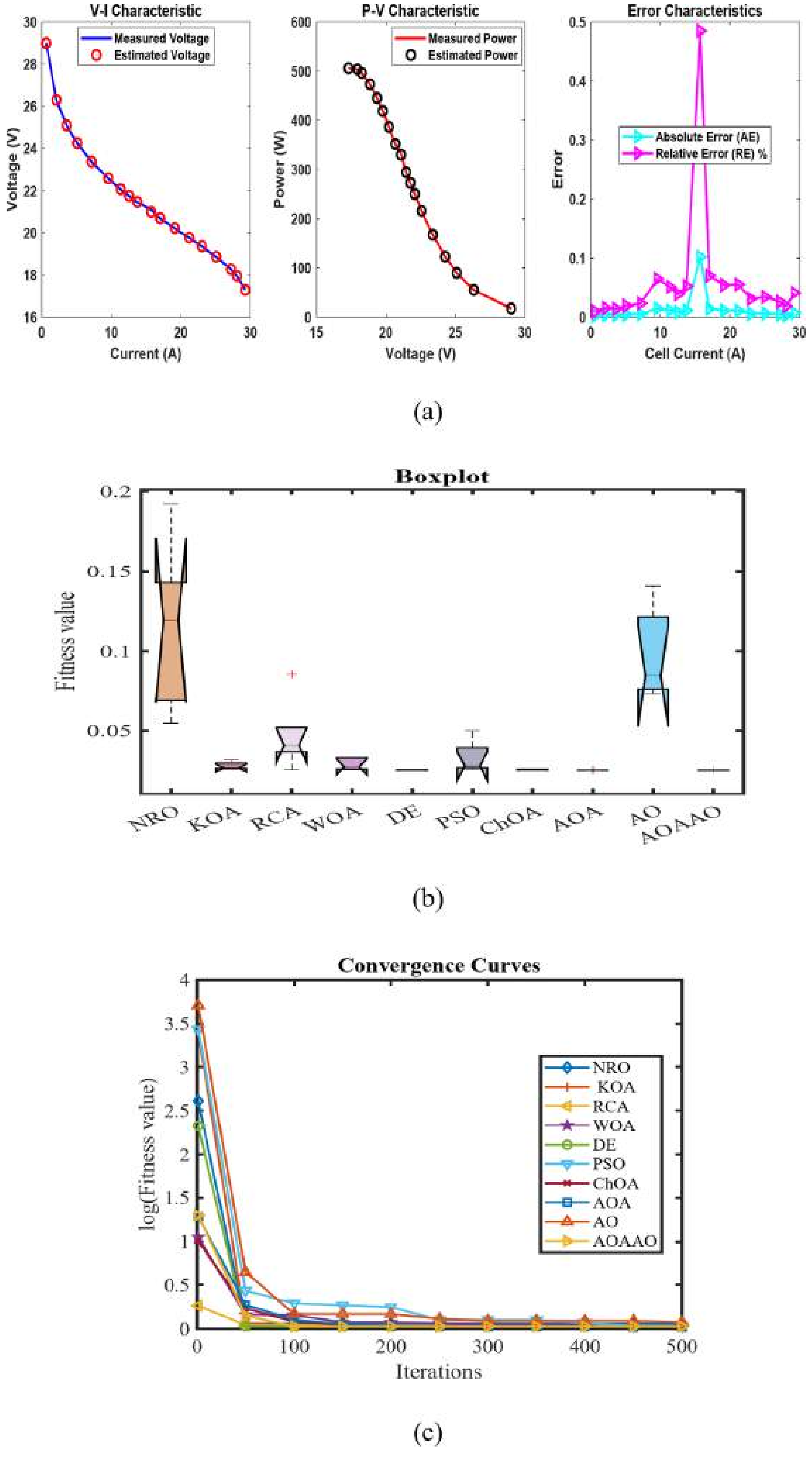

Fig. 3. AOAAO algorithm characteristic curves of Sheet 1; (**a**) V/I, P/V, and error curve, (**b**) Box-Plot, (**c**) Convergence Curve for Sheet 1.

Friedman ranking of 2.2, compared to other algorithms, confirms its superior performance across all evaluation metrics. Table 10 provides a detailed comparison of experimental and calculated values, while Fig. 5 illustrates the I/V and P/V curves, error curves, convergence curves, and box plots, visually demonstrating AOAAO exceptional performance and its significant advantage over other algorithms.

Algorithm	NRO	KOA	RCA	WOA	DE	PSO	ChOA	AOA	AO	AOAAO
ξ_1	− 1.10315	− 0.8532	− 1.15235	− 0.96635	− 0.87151	− 0.8532	− 0.88116	− 1.08097	− 0.8968	− 0.85498
ξ_2	0.003835	0.002397	0.00327	0.002858	0.002482	0.002532	0.003005	0.003235	0.002763	0.002438
ξ_3	8.64E-05	3.6E-05	0.000036	4.54E-05	3.82E-05	4.55E-05	7.35E-05	4.84E-05	5.21E-05	3.85E-05
ξ_4	− 9.5E-05	− 9.5E-05	− 9.5E-05	− 9.5E-05	− 9.5E-05	− 9.5E-05	− 9.5E-05	− 9.5E-05	− 9.5E-05	− 9.5E-05
λ	15.53654	14	14	14	14.00135	14	14	14.00281	21.81007	14
R_c	0.0001	0.000103	0.00012	0.000106	0.00012	0.000121	0.000123	0.000108	0.000399	0.00012
B	0.03593	0.019297	0.016788	0.018753	0.01698	0.016909	0.016248	0.018615	0.026352	0.016788
Min.	0.29739	0.275746	0.275211	0.275581	0.275228	0.275346	0.275305	0.275762	0.334858	0.275211
Max.	0.837166	0.319379	0.320685	0.295621	0.286627	0.300545	0.276626	0.285955	0.467356	0.275211
Mean	0.494496	0.292274	0.284815	0.281789	0.281106	0.281489	0.275946	0.278785	0.416984	0.275211
Std.	0.215484	0.017628	0.020055	0.008152	0.004777	0.010691	0.000477	0.004319	0.05035	5.84E-16
RT	4.627648	4.904398	4.362912	4.579656	8.922547	4.986948	5.036286	5.650808	9.583003	0.193296
FR	9.6	6.8	4	5.2	5.2	5.4	3.8	4.6	9.4	1

Table 7. Optimized parameters and optimal function value for sheet 2.

S_NO	Icell	Vcell	Vest	Pref	Pest	AE	RE %	MBE
1	2.25	61.64	62.32708	138.69	140.2359	0.687083	1.114671	0.016279
2	6.75	59.57	59.75391	402.0975	403.3389	0.183906	0.308722	0.001166
3	9	58.94	59.02299	530.46	531.207	0.082995	0.140813	0.000238
4	15.75	57.54	57.47245	906.255	905.191	0.067553	0.117401	0.000157
5	20.25	56.8	56.69501	1150.2	1148.074	0.104994	0.184848	0.00038
6	24.75	56.13	56.02304	1389.218	1386.57	0.106962	0.190562	0.000395
7	31.5	55.23	55.13803	1739.745	1736.848	0.091967	0.166516	0.000292
8	36	54.66	54.60299	1967.76	1965.708	0.057007	0.104294	0.000112
9	45	53.61	53.61886	2412.45	2412.849	0.008863	0.016533	2.71E-06
10	51.75	52.86	52.93264	2735.505	2739.264	0.072643	0.137426	0.000182
11	67.5	51.91	51.43559	3503.925	3471.902	0.474414	0.913916	0.007761
12	72	51.22	51.02539	3687.84	3673.828	0.194606	0.379942	0.001306
13	90	49.66	49.42672	4469.4	4448.405	0.233283	0.46976	0.001877
14	99	49	48.64101	4851	4815.46	0.358993	0.732639	0.004444
15	105.8	48.15	48.04916	5094.27	5083.601	0.100837	0.209422	0.000351
16	110.3	47.52	47.6574	5241.456	5256.611	0.137396	0.289134	0.000651
17	117	47.1	47.07283	5510.7	5507.521	0.02717	0.057687	2.55E-05
18	126	46.48	46.28306	5856.48	5831.665	0.196943	0.423715	0.001337
19	135	45.66	45.4853	6164.1	6140.516	0.174696	0.382603	0.001052
20	141.8	44.85	44.87551	6359.73	6363.347	0.025509	0.056876	2.24E-05
21	150.8	44.24	44.05684	6671.392	6643.772	0.183157	0.414008	0.001157
22	162	42.45	43.01569	6876.9	6968.542	0.565692	1.332607	0.011035
23	171	41.66	42.15751	7123.86	7208.934	0.49751	1.194214	0.008535
24	182.3	40.68	41.04751	7415.964	7482.96	0.367506	0.903408	0.004657
25	189	40.09	40.36954	7577.01	7629.843	0.279538	0.697275	0.002695
26	195.8	39.51	39.66413	7736.058	7766.236	0.154127	0.390097	0.000819
27	204.8	38.73	38.69983	7931.904	7925.726	0.030168	0.077892	3.14E-05
28	211.5	38.15	37.95577	8068.725	8027.646	0.194228	0.509117	0.001301
29	220.5	37.38	36.91421	8242.29	8139.583	0.465791	1.246096	0.007481
						0.211225	0.453869	0.002612

Table 8. Performance metrics of AOAAO algorithm for sheet 2.

SHEET 4: H-12-1 parameter optimization

AOAAO outperforms other differential evolution algorithms in terms of stability, precision, and computational efficiency. A detailed analysis of the metrics in Table 11 reveals that AOAAO consistently records the lowest minimum, maximum, mean, and standard deviation values. For example, AOAAO's minimum value of 0.102915 is lower than AOA, AO and remaining compared algorithms indicating superior predictability and minimal error margins. Additionally, AOAAO's maximum value of 0.102915 is lower than AOA and AO. The

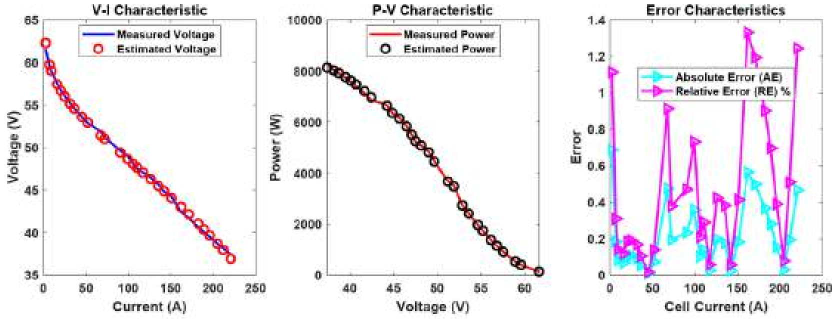

(a)

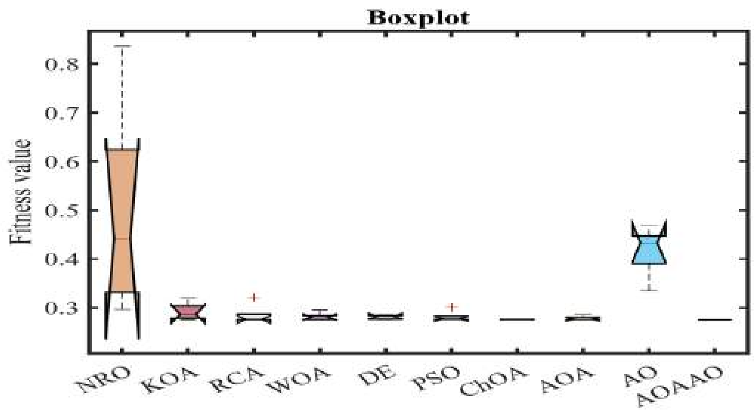

(b)

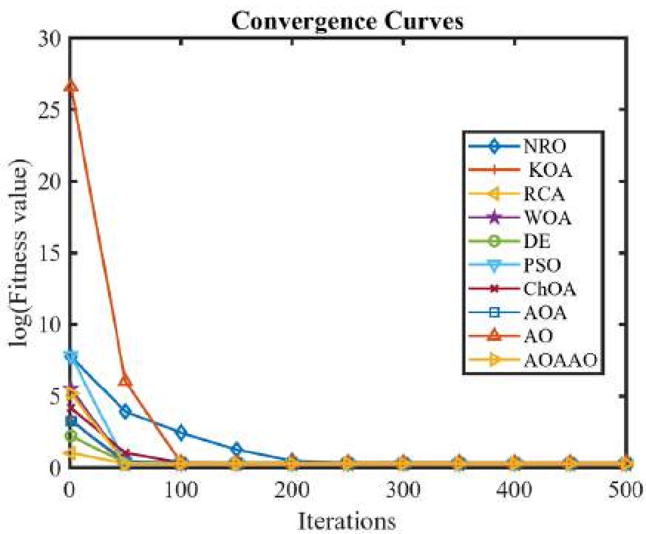

(c)

Fig. 4. AOAAO algorithm characteristic curves of Sheet 2; (**a**) V/I, P/V, and error curve, (**b**) Box-Plot, (**c**) convergence curve for Sheet 2.

standard deviation for AOAAO is almost negligible at 3.8E-17, reflecting less variability compared to AOA and AO. In terms of computational efficiency, AOAAO runtime of 0.132648 s is significantly faster than all compared algorithms, demonstrating an efficiency improvement of approximately 98%. Furthermore, AOAAO highest Friedman ranking of 1, compared to other algorithms, confirms its superior performance across all evaluation metrics. Table 12 provides a detailed comparison of experimental and calculated values, while Fig. 6 illustrates

Algorithm	NRO	KOA	RCA	WOA	DE	PSO	ChOA	AOA	AO	AOAAO
ξ_1	− 1.19268	− 0.86141	− 0.8532	− 1.03159	− 0.88797	− 0.9303	− 1.02158	− 0.94242	− 0.91562	− 0.89596
ξ_2	0.003894	0.003273	0.003251	0.003157	0.003026	0.002725	0.003539	0.00283	0.002571	0.002421
ξ_3	7.19E-05	9.78E-05	0.000098	5.65E-05	7.67E-05	4.86E-05	8.31E-05	5.31E-05	4.13E-05	3.6E-05
ξ_4	− 9.5E-05	− 9.5E-05	− 9.5E-05	− 9.5E-05	− 9.5E-05	− 9.5E-05	− 9.5E-05	− 9.5E-05	− 9.6E-05	− 9.5E-05
λ	23	22.69424	23	19.66628	22.97157	14.84181	22.79868	22.81813	18.93848	23
R_c	0.0001	0.000783	0.0008	0.000603	0.000671	0.000733	0.000646	0.000666	0.000541	0.000673
B	0.189474	0.173043	0.172796	0.175583	0.17533	0.170209	0.175742	0.175405	0.177995	0.17532
Min.	0.260359	0.242641	0.242716	0.242443	0.242286	0.243937	0.242365	0.242293	0.25835	0.242284
Max.	0.666933	0.245315	0.246387	0.245921	0.242614	0.248789	0.242628	0.242529	0.57641	0.242927
Mean	0.395458	0.243985	0.244869	0.243497	0.242418	0.245324	0.242493	0.242421	0.438272	0.242413
Std.	0.171831	0.001088	0.00133	0.001408	0.000136	0.001984	0.000111	8.47E-05	0.15043	0.000288
RT	3.533942	3.972945	3.021226	3.292506	7.074326	3.748679	3.75932	4.367551	6.982553	0.138754
FR	9.4	5.8	7	5.4	2.6	7.2	3.2	2.6	9.6	2.2

Table 9. Optimized parameters and optimal function value for sheet 3.

S_NO	Icell	Vcell	Vest	Pref	Pest	AE	RE%	MBE
1	1.004	43.17	43.34081	43.34268	43.51417	0.170809	0.395667	0.001621
2	3.166	41.14	41.09008	130.2492	130.0912	0.049922	0.121347	0.000138
3	5.019	40.09	39.91451	201.2117	200.3309	0.175488	0.437735	0.001711
4	7.027	39.04	38.85715	274.3341	273.0492	0.182848	0.46836	0.001857
5	8.958	37.99	37.93346	340.3144	339.808	0.056535	0.148816	0.000178
6	10.97	37.08	37.01454	406.7676	406.0495	0.065463	0.176546	0.000238
7	13.05	36.03	36.07991	470.1915	470.8428	0.049906	0.138511	0.000138
8	15.06	35.19	35.17136	529.9614	529.6807	0.018636	0.052958	1.93E-05
9	17.07	34.07	34.24209	581.5749	584.5124	0.172088	0.505102	0.001645
10	19.07	33.02	33.28313	629.6914	634.7092	0.263126	0.796869	0.003846
11	21.08	32.04	32.2707	675.4032	680.2664	0.2307	0.720038	0.002957
12	23.01	31.2	31.23769	717.912	718.7793	0.037694	0.120813	7.89E-05
13	24.94	29.8	30.12737	743.212	751.3766	0.327372	1.098562	0.005954
14	26.87	28.96	28.91713	778.1552	777.0034	0.042866	0.148018	0.000102
15	28.96	28.12	27.45776	814.3552	795.1766	0.662243	2.355061	0.024365
16	30.81	26.3	25.9918	810.303	800.8075	0.308195	1.171846	0.005277
17	32.97	24.06	23.98487	793.2582	790.7811	0.075131	0.312265	0.000314
18	34.9	21.4	21.78563	746.86	760.3186	0.385634	1.802028	0.008262
						0.181925	0.609475	0.003261

Table 10. Performance metrics of AOAAO algorithm for sheet 3.

the I/V and P/V curves, error curves, convergence curves, and box plots, visually demonstrating AOAAO exceptional performance and its significant advantage over other algorithms.

SHEET 5: Ballard Mark V parameter optimization

AOAAO outperforms other differential evolution algorithms in terms of stability, precision, and computational efficiency. A detailed analysis of the metrics in Table 13 reveals that AOAAO consistently records the lowest minimum, maximum, mean, and standard deviation values. For example, AOAAO's minimum value of 0.148632 is lower than AOA, AO and remaining compared algorithms indicating superior predictability and minimal error margins. Additionally, AOAAO's maximum value of 0.148632 is lower than AOA and AO. The standard deviation for AOAAO is almost negligible at 4.2E-16, reflecting less variability compared to AOA and AO. In terms of computational efficiency, AOAAO runtime of 0.122756 s is significantly faster than all compared algorithms, demonstrating an efficiency improvement of approximately 98%. Furthermore, AOAAO highest Friedman ranking of 1, compared to other algorithms, confirms its superior performance across all evaluation metrics. Table 14 provides a detailed comparison of experimental and calculated values, while Fig. 7 illustrates the I/V and P/V curves, error curves, convergence curves, and box plots, visually demonstrating AOAAO exceptional performance and its significant advantage over other algorithms.

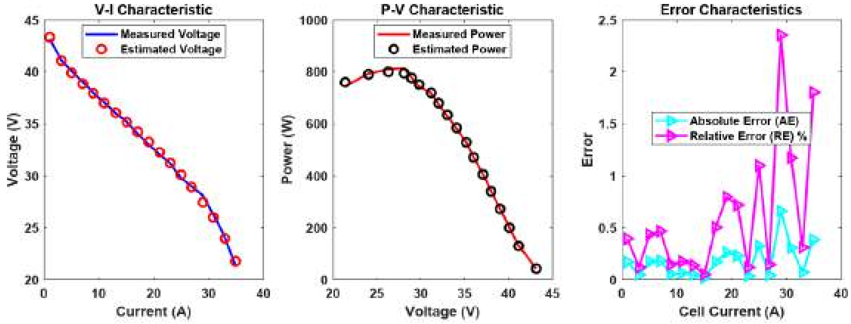

(a)

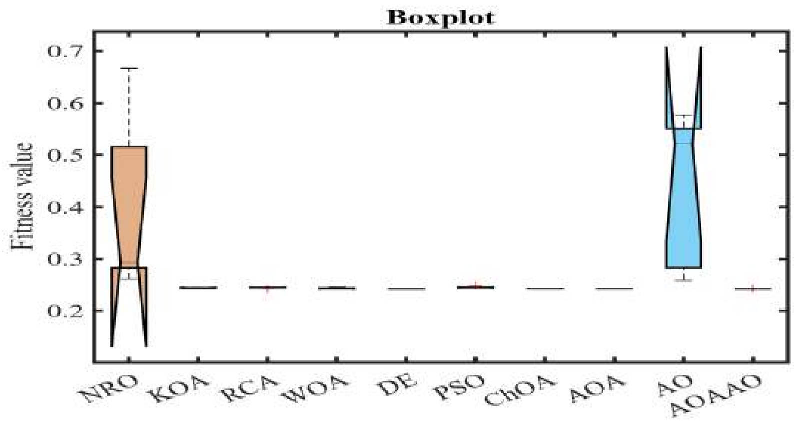

(b)

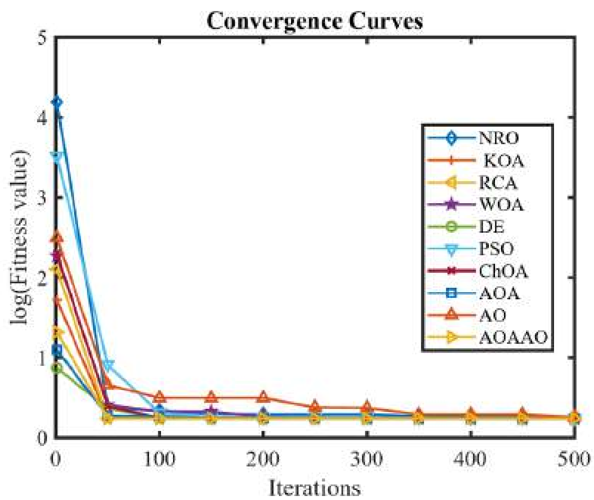

(c)

Fig. 5. AOAAO algorithm characteristic curves of Sheet 3; (**a**) V/I, P/V, and error curve, (**b**) Box-Plot, (**c**) convergence curve for Sheet 3.

SHEET 6: STD-1 parameter optimization

AOAAO outperforms other differential evolution algorithms in terms of stability, precision, and computational efficiency. A detailed analysis of the metrics in Table 15 reveals that AOAAO consistently records the lowest minimum, maximum, mean, and standard deviation values. For example, AOAAO's minimum value of 0.283774 is lower than AOA, AO and remaining compared algorithms indicating superior predictability and minimal error margins. Additionally, AOAAO's maximum value of 0.283774 is lower than AOA and AO. The standard

Algorithm	NRO	KOA	RCA	WOA	DE	PSO	ChOA	AOA	AO	AOAAO
ξ_1	− 1.1991	− 0.85741	− 1.19969	− 0.99876	− 0.98961	− 0.87395	− 0.86989	− 1.10522	− 1.19969	− 1.0506
ξ_2	0.002579	0.00188	0.003445	0.002693	0.002003	0.002408	0.002133	0.00302	0.002736	0.002454
ξ_3	3.6E-05	6.17E-05	0.000098	8.87E-05	4.12E-05	9.6E-05	7.72E-05	8.85E-05	4.72E-05	6E-05
ξ_4	− 0.00011	− 0.00011	− 0.00011	− 0.00011	− 0.00011	− 0.00011	− 0.00011	− 0.00011	− 0.00012	− 0.00011
λ	14	14	14	14.05763	14	14	14	14.00338	14.61221	14
R_c	0.0008	0.0008	0.0008	0.000661	0.0008	0.000509	0.0008	0.0008	0.000798	0.0008
B	0.0136	0.0136	0.0136	0.013616	0.0136	0.013865	0.0136	0.013601	0.013759	0.0136
Min.	0.102915	0.102915	0.102915	0.103076	0.102915	0.103278	0.102915	0.102916	0.103973	0.102915
Max.	0.107645	0.103578	0.104428	0.103905	0.10345	0.104292	0.102915	0.102919	0.108593	0.102915
Mean	0.104622	0.103245	0.103665	0.103397	0.103069	0.103677	0.102915	0.102918	0.106491	0.102915
Std.	0.001938	0.000314	0.000757	0.000334	0.00023	0.000402	2.72E-07	1E-06	0.002025	3.8E-17
RT	3.492326	3.325675	3.040772	3.733247	7.009067	3.519394	3.71745	4.248168	6.664965	0.132648
FR	7.4	5	5.6	7	5.2	7	2.8	4.2	9.8	1

Table 11. Optimized parameters and optimal function value for sheet 4.

S_NO	Icell	Vcell	Vest	Pref	Pest	AE	RE %	MBE
1	0.104	9.58	9.755532	0.99632	1.014575	0.175532	1.832272	0.001712
2	0.2	9.42	9.435534	1.884	1.887107	0.015534	0.164909	1.34E-05
3	0.309	9.25	9.215306	2.85825	2.84753	0.034694	0.37507	6.69E-05
4	0.403	9.2	9.075995	3.7076	3.657626	0.124005	1.347879	0.000854
5	0.51	9.09	8.947893	4.6359	4.563425	0.142107	1.563338	0.001122
6	0.614	8.95	8.842715	5.4953	5.429427	0.107285	1.19872	0.000639
7	0.703	8.85	8.762861	6.22155	6.160291	0.087139	0.984618	0.000422
8	0.806	8.74	8.678685	7.04444	6.99502	0.061315	0.70154	0.000209
9	0.908	8.65	8.601587	7.8542	7.810241	0.048413	0.559683	0.00013
10	1.076	8.45	8.483394	9.0922	9.128131	0.033394	0.39519	6.2E-05
11	1.127	8.41	8.448867	9.47807	9.521873	0.038867	0.462156	8.39E-05
12	1.288	8.2	8.341384	10.5616	10.7437	0.141384	1.724194	0.001111
13	1.39	8.12	8.272663	11.2868	11.499	0.152663	1.880081	0.001295
14	1.45	8.11	8.231198	11.7595	11.93524	0.121198	1.494432	0.000816
15	1.578	8.05	8.137515	12.7029	12.841	0.087515	1.087138	0.000425
16	1.707	7.99	8.028856	13.63893	13.70526	0.038856	0.486306	8.39E-05
17	1.815	7.95	7.912602	14.42925	14.36137	0.037398	0.47041	7.77E-05
18	1.9	7.94	7.777413	15.086	14.77708	0.162587	2.047696	0.001469
						0.089438	1.043091	0.000588

Table 12. Performance metrics of AOAAO algorithm for sheet 4.

deviation for AOAAO is almost negligible at 8.33E-17, reflecting less variability compared to AOA and AO. In terms of computational efficiency, AOAAO runtime of 0.108746 s is significantly faster than all compared algorithms, demonstrating an efficiency improvement of approximately 98%. Furthermore, AOAAO highest Friedman ranking of 1, compared to other algorithms, confirms its superior performance across all evaluation metrics. Table 16 provides a detailed comparison of experimental and calculated values, while Fig. 8 illustrates the I/V and P/V curves, error curves, convergence curves, and box plots, visually demonstrating AOAAO exceptional performance and its significant advantage over other algorithms.

SHEET 7: horizon parameter optimization

AOAAO outperforms other differential evolution algorithms in terms of stability, precision, and computational efficiency. A detailed analysis of the metrics in Table 17 reveals that AOAAO consistently records the lowest minimum, maximum, mean, and standard deviation values. For example, AOAAO's minimum value of 0.121755 is lower than AOA, AO and remaining compared algorithms indicating superior predictability and minimal error margins. Additionally, AOAAO's maximum value of 0.121755 is lower than AOA and AO. The standard deviation for AOAAO is almost negligible at 1.63E-16, reflecting less variability compared to AOA and AO. In terms of computational efficiency, AOAAO runtime of 0.117998 s is significantly faster than all compared algorithms, demonstrating an efficiency improvement of approximately 98%. Furthermore, AOAAO highest Friedman ranking of 1, compared to other algorithms, confirms its superior performance across all evaluation metrics. Table 18 provides a detailed comparison of experimental and calculated values, while Fig. 9 illustrates

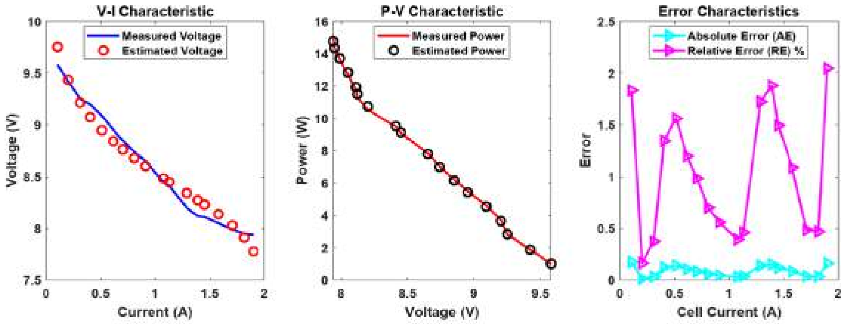

(a)

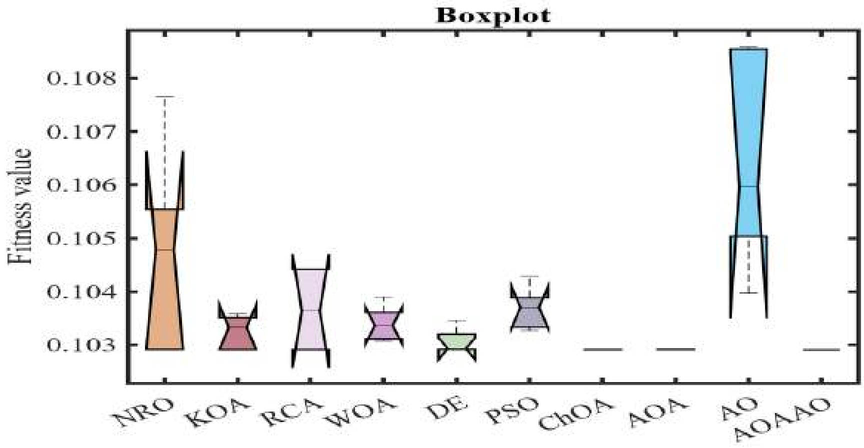

(b)

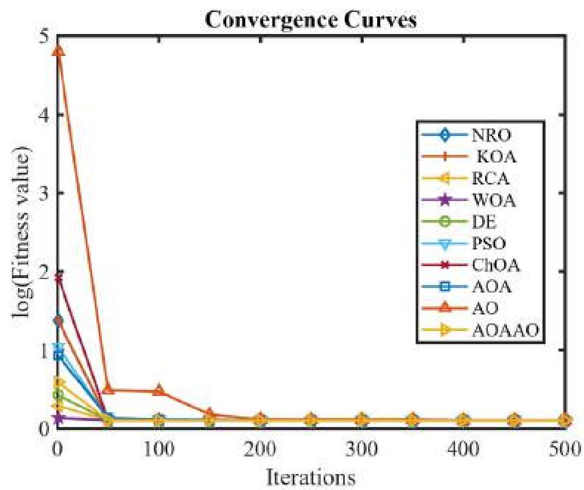

(c)

Fig. 6. AOAAO algorithm characteristic curves of Sheet 4; (**a**) V/I, P/V, and error curve, (**b**) Box-Plot, (**c**) convergence curve for Sheet 4.

the I/V and P/V curves, error curves, convergence curves, and box plots, visually demonstrating AOAAO exceptional performance and its significant advantage over other algorithms.

SHEET 8: STD-2 parameter optimization

AOAAO outperforms other differential evolution algorithms in terms of stability, precision, and computational efficiency. A detailed analysis of the metrics in Table 19 reveals that AOAAO consistently records the lowest

Algorithm	NRO	KOA	RCA	WOA	DE	PSO	ChOA	AOA	AO	AOAAO
ξ_1	− 1.04515	− 1.03065	− 1.19969	− 0.87553	− 0.90709	− 0.87803	− 1.09292	− 1.09967	− 0.87362	− 0.93829
ξ_2	0.003144	0.003174	0.004138	0.002598	0.002705	0.002581	0.003587	0.003165	0.002645	0.003169
ξ_3	5.96E-05	6.43E-05	0.000098	5.55E-05	5.66E-05	5.38E-05	8.09E-05	4.94E-05	6.01E-05	8.32E-05
ξ_4	− 0.00017	− 0.00018	− 0.00017	− 0.00017	− 0.00017	− 0.00017	− 0.00017	− 0.00017	− 0.00016	− 0.00017
λ	14.16512	16.28909	14.43912	14.63427	14.55899	14.68897	14.67389	14.462	14	14.43913
R_c	0.00011	0.000289	0.0001	0.000154	0.000144	0.000124	0.000125	0.0001	0.000575	0.0001
B	0.0136	0.016091	0.013795	0.013997	0.013816	0.014246	0.014071	0.01383	0.0136	0.013795
Min.	0.149733	0.150516	0.148632	0.148744	0.148718	0.148733	0.148727	0.148633	0.168511	0.148632
Max.	0.155617	0.155266	0.149959	0.151388	0.149417	0.151125	0.148811	0.148692	0.232626	0.148632
Mean	0.152059	0.152596	0.149069	0.149644	0.149067	0.150006	0.14876	0.148646	0.196065	0.148632
Std.	0.003012	0.001963	0.000602	0.001029	0.000293	0.000883	3.98E-05	2.56E-05	0.025611	4.2E-16
RT	2.987005	3.110125	2.637839	2.790597	5.537107	3.214418	3.347177	3.97236	5.799443	0.122756
FR	8	8.6	3.6	6	4.8	6.8	3.8	2.4	10	1

Table 13. Optimized parameters and optimal function value for sheet 5.

S_NO	Icell	Vcell	Vest	Pref	Pest	AE	RE %	MBE
1	0.5	23.5	23.48309	11.75	11.74154	0.016914	0.071975	1.91E-05
2	2.1	21.5	21.2513	45.15	44.62774	0.248696	1.156727	0.004123
3	2.8	20.5	20.75981	57.4	58.12748	0.259815	1.267389	0.0045
4	4	19.9	20.10958	79.6	80.43831	0.209577	1.053152	0.002928
5	5.7	19.5	19.39753	111.15	110.5659	0.102468	0.525477	0.0007
6	7.1	19	18.90725	134.9	134.2415	0.092746	0.488139	0.000573
7	8	18.5	18.61964	148	148.9571	0.11964	0.646705	0.000954
8	11.1	17.8	17.72275	197.58	196.7226	0.077246	0.433969	0.000398
9	13.7	17.3	17.02409	237.01	233.23	0.275911	1.594863	0.005075
10	16.5	16.2	16.27464	267.3	268.5316	0.074644	0.460763	0.000371
11	17.5	15.9	15.99828	278.25	279.9699	0.09828	0.618116	0.000644
12	18.9	15.5	15.59366	292.95	294.7201	0.093658	0.604245	0.000585
13	20.3	15.1	15.15114	306.53	307.5681	0.05114	0.338674	0.000174
14	22	14.6	14.47819	321.2	318.5201	0.121813	0.834336	0.000989
15	22.9	13.8	13.82904	316.02	316.685	0.029041	0.210444	5.62E-05
						0.124773	0.686998	0.001473

Table 14. Performance metrics of AOAAO algorithm for sheet 5.

minimum, maximum, mean, and standard deviation values. For example, AOAAO's minimum value of 0.078492 is lower than AOA, AO and remaining compared algorithms indicating superior predictability and minimal error margins. Additionally, AOAAO's maximum value of 0.078492 is lower than AOA and AO. The standard deviation for AOAAO is almost negligible at 7.17E-16, reflecting less variability compared to AOA and AO. In terms of computational efficiency, AOAAO runtime of 0.125494 s is significantly faster than all compared algorithms, demonstrating an efficiency improvement of approximately 98%. Furthermore, AOAAO highest Friedman ranking of 1.2, compared to other algorithms, confirms its superior performance across all evaluation metrics. Table 20 provides a detailed comparison of experimental and calculated values, while Fig. 10 illustrates the I/V and P/V curves, error curves, convergence curves, and box plots, visually demonstrating AOAAO exceptional performance and its significant advantage over other algorithms.

SHEET 9: STD-3 parameter optimization

AOAAO outperforms other differential evolution algorithms in terms of stability, precision, and computational efficiency. A detailed analysis of the metrics in Table 21 reveals that AOAAO consistently records the lowest minimum, maximum, mean, and standard deviation values. For example, AOAAO's minimum value of 0.202319 is lower than AOA, AO and remaining compared algorithms indicating superior predictability and minimal error margins. Additionally, AOAAO's maximum value of 0.202319 is lower than AOA and AO. The standard deviation for AOAAO is almost negligible at 2.46E-16, reflecting less variability compared to AOA and AO. In terms of computational efficiency, AOAAO runtime of 0.119009 s is significantly faster than all compared algorithms, demonstrating an efficiency improvement of approximately 98%. Furthermore, AOAAO highest Friedman ranking of 1, compared to other algorithms, confirms its superior performance across all evaluation metrics. Table 22 provides a detailed comparison of experimental and calculated values, while Fig. 11 illustrates

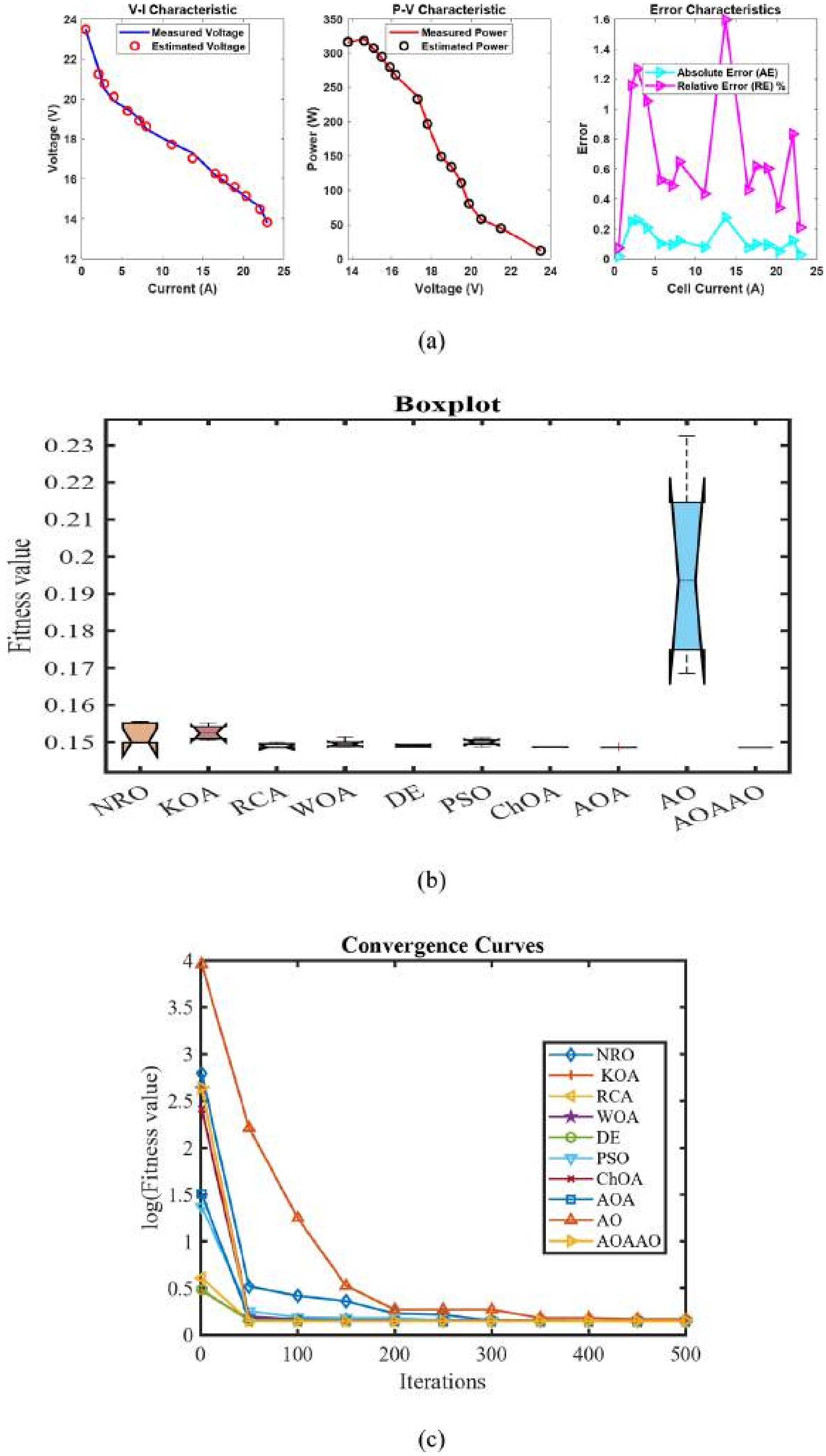

Fig. 7. AOAAO algorithm characteristic curves of Sheet 5; (**a**) V/I, P/V, and error curve, (**b**) Box-Plot, (**c**) Convergence Curve for Sheet 5.

the I/V and P/V curves, error curves, convergence curves, and box plots, visually demonstrating AOAAO exceptional performance and its significant advantage over other algorithms.

SHEET 10: STD-4 parameter optimization

AOAAO outperforms other differential evolution algorithms in terms of stability, precision, and computational efficiency. A detailed analysis of the metrics in Table 23 reveals that AOAAO consistently records the lowest

Algorithm	NRO	KOA	RCA	WOA	DE	PSO	ChOA	AOA	AO	AOAAO
ξ_1	− 0.99852	− 1.16337	− 0.8532	− 1.05312	− 1.0607	− 1.14097	− 0.92833	− 1.06531	− 1.10293	− 0.86344
ξ_2	0.002573	0.002951	0.002063	0.003216	0.002942	0.003056	0.002843	0.0032	0.002651	0.001914
ξ_3	5.48E-05	4.72E-05	4.93E-05	8.94E-05	6.83E-05	5.94E-05	8.92E-05	8.57E-05	3.82E-05	3.65E-05
ξ_4	− 0.00017	− 0.00017	− 0.00017	− 0.00017	− 0.00017	− 0.00017	− 0.00017	− 0.00017	− 0.00018	− 0.00017
λ	14	14	14	14	14.00001	15.90356	14	14.00036	14	14
R_c	0.0008	0.0008	0.0008	0.000799	0.0008	0.0008	0.0008	0.0008	0.000421	0.0008
B	0.016912	0.017314	0.017317	0.017211	0.017322	0.017493	0.01731	0.017287	0.015106	0.017317
Min.	0.284619	0.283774	0.283774	0.283864	0.283774	0.288423	0.283807	0.283779	0.337645	0.283774
Max.	0.344437	0.287801	0.297691	0.324159	0.283836	0.330287	0.283913	0.283806	0.353931	0.283774
Mean	0.304319	0.285126	0.294908	0.296998	0.283795	0.319987	0.283854	0.28379	0.346696	0.283774
Std.	0.026932	0.001742	0.006224	0.018609	2.77E-05	0.017708	4.55E-05	1.11E-05	0.006794	8.33E-17
RT	2.793698	2.749722	2.489156	2.366619	5.895762	3.425115	3.089692	4.15727	6.989436	0.108746
FR	7.6	4.6	6.4	6.2	3.2	8.6	4.4	3.2	9.8	1

Table 15. Optimized parameters and optimal function value for sheet 6.

S_NO	Icell	Vcell	Vest	Pref	Pest	AE	RE %	MBE
1	0.6	29.37	29.7147	17.622	17.82882	0.344698	1.17364	0.00914
2	2.5	26.77739	26.62879	66.94348	66.57198	0.148596	0.554931	0.001699
3	5	25.29025	25.00559	126.4513	125.0279	0.284663	1.125585	0.006233
4	7.5	24.28186	23.96352	182.1139	179.7264	0.318339	1.311014	0.007795
5	10	23.418	23.14754	234.18	231.4754	0.270455	1.154903	0.005627
6	12	22.7391	22.57673	272.8692	270.9208	0.162374	0.714072	0.002028
7	14	22.05852	22.04306	308.8193	308.6028	0.015467	0.070117	1.84E-05
8	16	21.38615	21.52088	342.1784	344.3341	0.134734	0.630007	0.001396
9	18	20.72173	20.98016	372.9911	377.6428	0.258429	1.247139	0.005137
10	20	20.026	20.364	400.52	407.28	0.337999	1.687803	0.008788
11	21	19.63635	19.98091	412.3634	419.5992	0.344565	1.75473	0.009133
12	22	19.19181	19.45678	422.2198	428.0492	0.264976	1.380673	0.005401
13	23	18.66363	18.17812	429.2635	418.0968	0.485508	2.60136	0.018132
						0.259293	1.185075	0.006194

Table 16. Performance metrics of AOAAO algorithm for sheet 6.

minimum, maximum, mean, and standard deviation values. For example, AOAAO's minimum value of 0.104446 is lower than AOA, AO and remaining compared algorithms indicating superior predictability and minimal error margins. Additionally, AOAAO's maximum value of 0.104446 is lower than AOA and AO. The standard deviation for AOAAO is almost negligible at 1.37E-16, reflecting less variability compared to AOA and AO. In terms of computational efficiency, AOAAO runtime of 0.113806 s is significantly faster than all compared algorithms, demonstrating an efficiency improvement of approximately 98%. Furthermore, AOAAO highest Friedman ranking of 1, compared to other algorithms, confirms its superior performance across all evaluation metrics. Table 24 provides a detailed comparison of experimental and calculated values, while Fig. 12 illustrates the I/V and P/V curves, error curves, convergence curves, and box plots, visually demonstrating AOAAO exceptional performance and its significant advantage over other algorithms.

SHEET 11: H-12-2 parameter optimization

AOAAO outperforms other differential evolution algorithms in terms of stability, precision, and computational efficiency. A detailed analysis of the metrics in Table 25 reveals that AOAAO consistently records the lowest minimum, maximum, mean, and standard deviation values. For example, AOAAO's minimum value of 0.075484 is lower than AOA, AO and remaining compared algorithms indicating superior predictability and minimal error margins. Additionally, AOAAO's maximum value of 0.076103 is lower than AOA and AO. The standard deviation for AOAAO is almost negligible at 0.000277, reflecting less variability compared to AOA and AO. In terms of computational efficiency, AOAAO runtime of 0.120014 s is significantly faster than all compared algorithms, demonstrating an efficiency improvement of approximately 98%. Furthermore, AOAAO highest Friedman ranking of 2.4, compared to other algorithms, confirms its superior performance across all evaluation metrics. Table 26 provides a detailed comparison of experimental and calculated values, while Fig. 13 illustrates the I/V and P/V curves, error curves, convergence curves, and box plots, visually demonstrating AOAAO exceptional performance and its significant advantage over other algorithms.

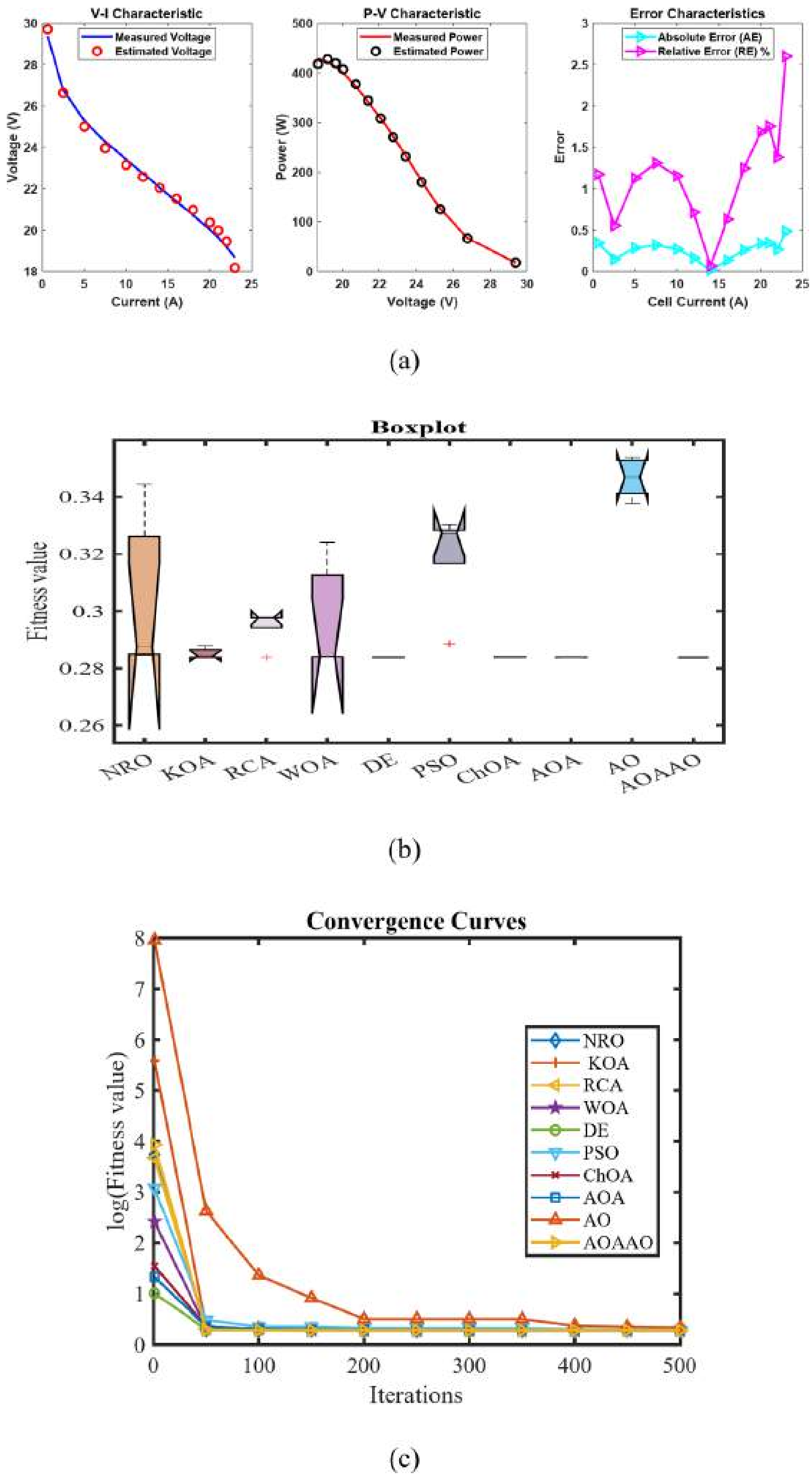

Fig. 8. AOAAO algorithm characteristic curves of Sheet 6; (**a**) V/I, P/V, and error curve, (**b**) box-plot, (**c**) convergence curve for Sheet 6.

SHEET 12: H-12-3 parameter optimization

AOAAO outperforms other differential evolution algorithms in terms of stability, precision, and computational efficiency. A detailed analysis of the metrics in Table 27 reveals that AOAAO consistently records the lowest minimum, maximum, mean, and standard deviation values. For example, AOAAO's minimum value of 0.064194 is lower than AOA, AO and remaining compared algorithms indicating superior predictability and minimal error margins. Additionally, AOAAO's maximum value of 0.064194 is lower than AOA and AO. The standard

Algorithm	NRO	KOA	RCA	WOA	DE	PSO	ChOA	AOA	AO	AOAAO
ξ_1	− 0.87556	− 0.92811	− 0.8532	− 0.87027	− 1.12252	− 0.85748	− 1.02352	− 0.93454	− 0.87942	− 0.8532
ξ_2	0.002882	0.002729	0.002681	0.002729	0.003637	0.002559	0.003018	0.00235	0.002448	0.002012
ξ_3	9.51E-05	7.27E-05	8.52E-05	8.51E-05	9.77E-05	7.53E-05	7.34E-05	4.35E-05	6.19E-05	3.6E-05
ξ_4	− 0.00015	− 0.00015	− 0.00015	− 0.00015	− 0.00015	− 0.00015	− 0.00015	− 0.00015	− 0.00014	− 0.00015
λ	21.31568	23	23	23	23	21.46314	23	22.99889	16.5934	23
R_c	0.0001	0.000101	0.0001	0.000111	0.0001	0.000105	0.00011	0.0001	0.0001	0.0001
B	0.050954	0.050976	0.050979	0.051025	0.050978	0.049767	0.051033	0.050986	0.042613	0.050979
Min.	0.126738	0.121772	0.121755	0.121913	0.121755	0.124627	0.121936	0.121758	0.172529	0.121755
Max.	0.172989	0.126173	0.134718	0.125746	0.1219	0.127081	0.122979	0.12177	0.251789	0.121755
Mean	0.147524	0.123981	0.132125	0.123292	0.121802	0.125732	0.122436	0.121763	0.198104	0.121755
Std.	0.017493	0.001757	0.005797	0.001589	6.3E-05	0.001095	0.000443	5.08E-06	0.031528	1.63E-16
RT	2.991214	2.952264	2.527843	2.724012	6.063437	3.161635	4.918367	4.713127	5.994351	0.117998
FR	9	5.8	6.8	5.2	2.8	6.8	5	2.6	10	1

Table 17. Optimized parameters and optimal function value for sheet 7.

S_NO	Icell	Vcell	Vest	Pref	Pest	AE	RE %	MBE
1	0.2417	22.6916	22.56459	5.48456	5.453861	0.127013	0.559736	0.001075
2	1.3177	20.1869	20.35845	26.60028	26.82634	0.171555	0.849833	0.001962
3	2.6819	19.2897	19.32465	51.73305	51.82677	0.034945	0.18116	8.14E-05
4	4.0118	18.5607	18.66664	74.46182	74.88683	0.105942	0.570787	0.000748
5	5.3755	18.1682	18.13216	97.66316	97.46943	0.03604	0.198369	8.66E-05
6	6.7563	17.7196	17.66513	119.7189	119.3509	0.054469	0.307396	0.000198
7	8.0689	17.271	17.26039	139.358	139.2724	0.010608	0.06142	7.5E-06
8	10.8134	16.4299	16.47265	177.6631	178.1254	0.042753	0.260212	0.000122
9	13.4556	15.7009	15.72573	211.265	211.5991	0.02483	0.158146	4.11E-05
10	16.1488	14.9907	14.90759	242.0818	240.7397	0.083107	0.554389	0.00046
11	17.5295	14.6542	14.43437	256.8808	253.0272	0.219834	1.500145	0.003222
12	18.8423	14.0374	13.92017	264.4969	262.288	0.117233	0.835145	0.000916
13	20.2234	13.1963	13.25588	266.8741	268.079	0.059584	0.45152	0.000237
14	21.6049	12.0187	12.30085	259.6628	265.7587	0.282153	2.347615	0.005307
15	22.9189	10.1308	10.05734	232.1868	230.5032	0.073458	0.725094	0.00036
						0.096235	0.637398	0.000988

Table 18. Performance metrics of AOAAO algorithm for sheet 7.

deviation for AOAAO is almost negligible at 1.31E-16, reflecting less variability compared to AOA and AO. In terms of computational efficiency, AOAAO runtime of 0.129202 s is significantly faster than all compared algorithms, demonstrating an efficiency improvement of approximately 98%. Furthermore, AOAAO highest Friedman ranking of 1.2, compared to other algorithms, confirms its superior performance across all evaluation metrics. Table 28 provides a detailed comparison of experimental and calculated values, while Fig. 14 illustrates the I/V and P/V curves, error curves, convergence curves, and box plots, visually demonstrating AOAAO exceptional performance and its significant advantage over other algorithms.

Conclusion

Due to the inherent complexity and non-linearity of PEMFC systems, precise parameter estimation is crucial for accurate modeling, design, and control. V/I and P/V characteristics, influenced by operating temperature and gas pressure, provide valuable insights for parameter identification. This work investigates twelve different PEMFCs based on datasheet specifications, utilizing the recently developed hybrid AOAAO algorithm. The performance of AOAAO is compared to state-of-the-art algorithms like NRO, KOA, RCA, WOA, DE, PSO, ChOA, AOA, and AO to assess its numerical and statistical superiority.

- Superior Convergence: AOAAO effectively optimizes the seven nonlinear parameters of the PEMFC stack model, achieving convergence that closely aligns with experimental data across various cases.
- Enhanced Accuracy in Error Metrics: Beyond SSE, AOAAO also minimized the average values of Absolute Error (AE), Relative Error (RE), and Mean Bias Error (MBE), outperforming other compared algorithms in all cases, showcasing its consistency and accuracy.

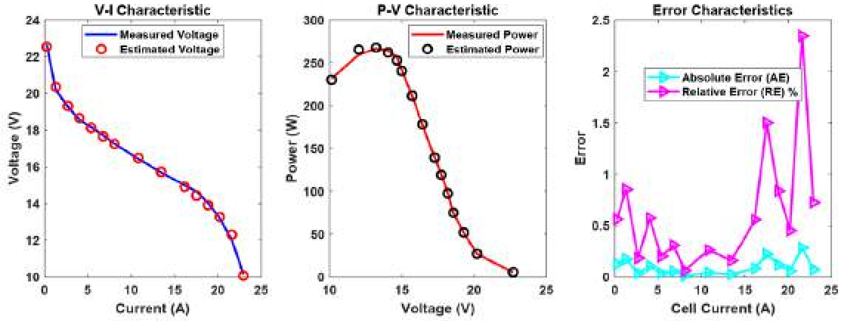

(a)

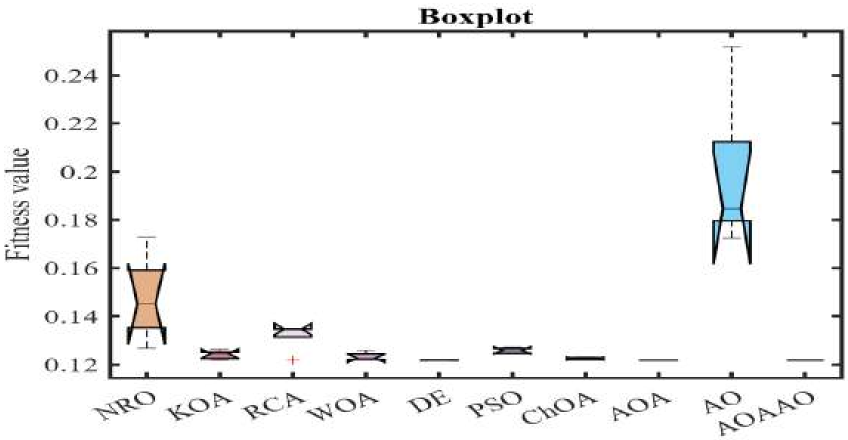

(b)

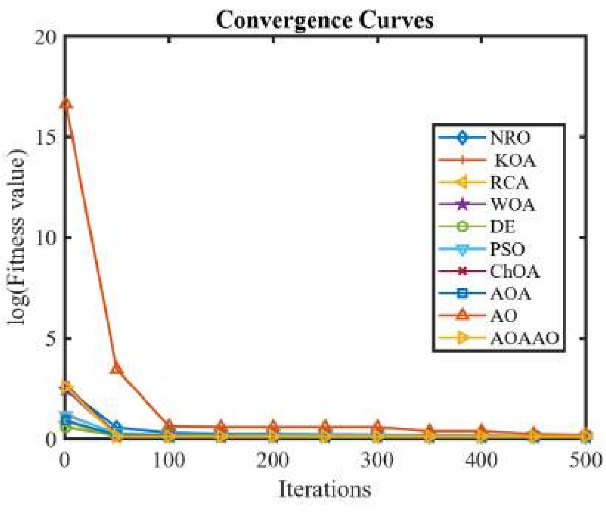

(c)

Fig. 9. AOAAO algorithm characteristic curves of Sheet 7; (**a**) V/I, P/V, and error curve, (**b**) box-plot, (**c**) convergence curve for Sheet 7.

- Alignment with Experimental I/V and P/V Curves: Optimized parameter settings obtained with AOAAO consistently aligned the I/V and P/V curves with experimental data across all PEMFC cases, affirming the model's reliability.

In terms of computational efficiency, AOAAO runtime is significantly faster than all compared algorithms, demonstrating an efficiency improvement of approximately 98%. These findings establish AOAAO as a highly

Algorithm	NRO	KOA	RCA	WOA	DE	PSO	ChOA	AOA	AO	AOAAO
ξ_1	− 0.8747	− 1.09779	− 1.01886	− 0.97389	− 0.85949	− 0.94628	− 0.94866	− 1.04921	− 0.87878	− 1.01075
ξ_2	0.002573	0.003446	0.002526	0.002721	0.002286	0.002348	0.002772	0.002802	0.002612	0.003294
ξ_3	7.21E-05	8.94E-05	0.000036	6.13E-05	5.34E-05	3.85E-05	7.09E-05	5.05E-05	7.4E-05	9.73E-05
ξ_4	− 0.00015	− 0.00015	− 0.00015	− 0.00015	− 0.00015	− 0.00015	− 0.00015	− 0.00015	− 0.00015	− 0.00015
λ	14.95413	15.54535	14.39771	14.78645	14.39901	14.22498	14.23262	14.40336	17.56663	14.39771
R_c	0.0001	0.000354	0.0001	0.00011	0.0001	0.000128	0.0001	0.0001	0.000666	0.0001
B	0.025112	0.025083	0.023974	0.024721	0.023977	0.023081	0.023596	0.023979	0.02836	0.023974
Min.	0.079457	0.079873	0.078492	0.078926	0.078492	0.079398	0.078603	0.078493	0.095963	0.078492
Max.	0.08955	0.087016	0.17633	0.084189	0.0806	0.094094	0.078996	0.078537	0.231545	0.078492
Mean	0.084973	0.082306	0.104625	0.081047	0.079047	0.083266	0.078832	0.078506	0.151751	0.078492
Std.	0.003651	0.002798	0.041783	0.002035	0.000886	0.006179	0.000168	1.82E-05	0.054874	7.17E-16
RT	3.076646	3.089659	2.573817	2.794122	5.645827	3.206694	3.33847	4.038665	5.965567	0.125494
FR	7.8	7.2	6.8	5.8	3.8	6.4	4	2.4	9.6	1.2

Table 19. Optimized parameters and optimal function value for sheet 8.

S_NO	Icell	Vcell	Vest	Pref	Pest	AE	RE %	MBE
1	0.2582	23.271	23.21664	6.008572	5.994536	0.054362	0.233603	0.000197
2	1.334	21.028	21.10731	28.05135	28.15715	0.07931	0.377162	0.000419
3	2.6471	20.0748	20.11794	53.14	53.2542	0.043141	0.214901	0.000124
4	4.0281	19.4019	19.43404	78.15279	78.28224	0.032136	0.165632	6.88E-05
5	5.3919	18.8972	18.90022	101.8918	101.9081	0.003018	0.015969	6.07E-07
6	6.7726	18.5047	18.4333	125.3249	124.8413	0.071404	0.385869	0.00034
7	8.0852	18.0561	18.02927	145.9872	145.7702	0.026832	0.148601	4.8E-05
8	10.8297	17.2897	17.24932	187.2423	186.805	0.040375	0.233523	0.000109
9	13.523	16.5047	16.51247	223.1931	223.2982	0.007774	0.047103	4.03E-06
10	16.1652	15.7196	15.76837	254.1105	254.8989	0.048774	0.310273	0.000159
11	17.5459	15.3271	15.35272	268.9278	269.3773	0.025619	0.167146	4.38E-05
12	18.8584	14.9907	14.92473	282.7006	281.4565	0.06597	0.440075	0.00029
13	20.2733	14.5421	14.39848	294.8164	291.9046	0.143623	0.987639	0.001375
14	21.5523	13.5888	13.79568	292.8699	297.3287	0.206881	1.522436	0.002853
15	22.9337	12.5234	12.47931	287.2079	286.1969	0.044085	0.352021	0.00013
						0.059554	0.373464	0.000411

Table 20. Performance metrics of AOAAO algorithm for sheet 8.

suitable approach for implementation in electronic component simulators for analyzing and studying PEMFC devices, given its precision, robustness, and computational efficiency.

Future work

Future research avenues include expanding the AOAAO algorithm's applicability to diverse fuel cell technologies, such as SOFCs, to evaluate its robustness and generalizability. Incorporating real-time data and dynamic environmental factors into the parameter estimation process would enhance the algorithm's adaptability to real-world conditions. Hybridizing AOAAO with machine learning techniques could enable predictive degradation modeling and optimized performance over the fuel cell's lifespan. Finally, integrating AOAAO into embedded systems would facilitate real-time control and monitoring of PEMFCs, paving the way for efficient, automated fuel cell management in practical applications.

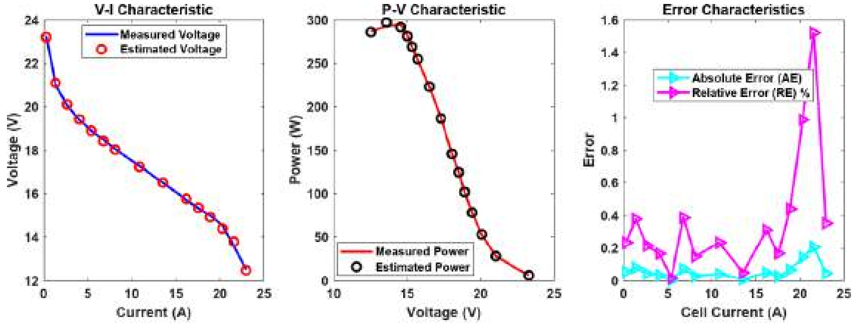

(a)

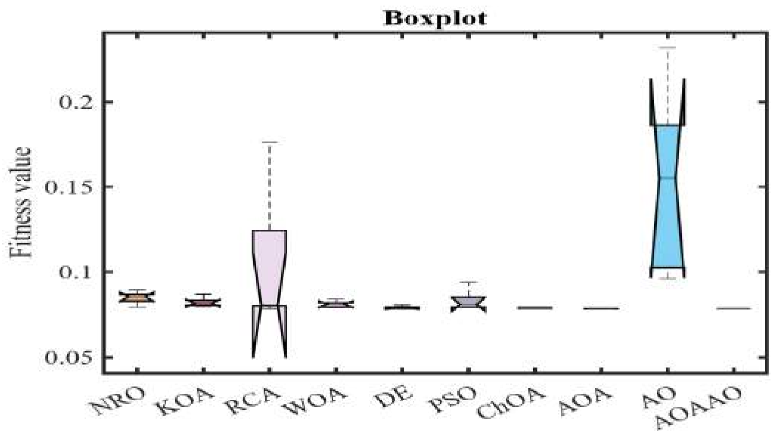

(b)

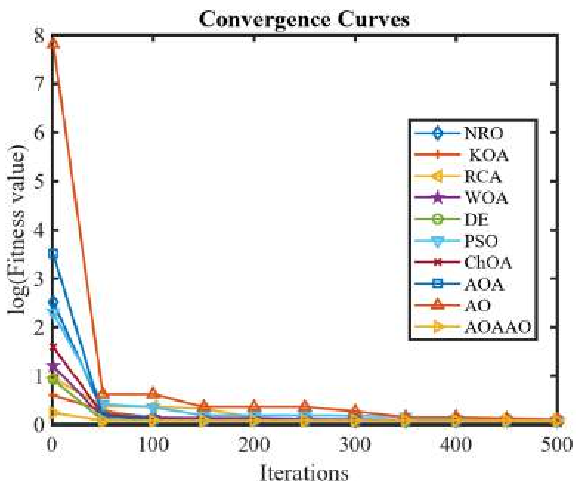

(c)

Fig. 10. AOAAO algorithm characteristic curves of Sheet 8; (**a**) V/I, P/V, and error curve, (**b**) Box-Plot, (**c**) convergence curve for Sheet 8.

Algorithm	NRO	KOA	RCA	WOA	DE	PSO	ChOA	AOA	AO	AOAAO
ξ_1	− 0.96034	− 0.86284	− 1.19713	− 1.19969	− 0.9616	− 1.07782	− 0.9736	− 1.13315	− 1.12959	− 0.85373
ξ_2	0.002883	0.001873	0.003394	0.002871	0.002334	0.003032	0.002259	0.002772	0.003155	0.002009
ξ_3	9.21E-05	3.62E-05	7.84E-05	3.74E-05	4.96E-05	7.74E-05	4.1E-05	4.47E-05	7.56E-05	4.87E-05
ξ_4	− 0.00012	− 0.00012	− 0.00012	− 0.00012	− 0.00012	− 0.00012	− 0.00012	− 0.00012	− 0.0001	− 0.00012
λ	23	23	23	22.72916	23	22.86822	22.77536	22.99932	18.80431	23
R_c	0.0001	0.0001	0.0001	0.000123	0.0001	0.000119	0.0001	0.0001	0.000445	0.0001
B	0.061758	0.06248	0.06248	0.062141	0.062458	0.06275	0.062385	0.062519	0.061749	0.06248
Min.	0.203049	0.202319	0.202319	0.202777	0.202321	0.202742	0.202566	0.202322	0.234648	0.202319
Max.	0.212686	0.205535	0.209699	0.208314	0.202769	0.206097	0.202854	0.202353	0.639658	0.202319
Mean	0.207405	0.204347	0.205271	0.204831	0.202429	0.20436	0.202685	0.202331	0.369035	0.202319
Std.	0.003712	0.001275	0.004042	0.002089	0.000191	0.001481	0.000108	1.25E-05	0.179347	2.46E-16
RT	3.070509	3.104423	2.557149	2.833461	5.674072	3.235931	3.34459	3.919318	6.098795	0.119009
FR	7.8	6	4.8	7.2	3.8	6.8	4.6	3	10	1

Table 21. Optimized parameters and optimal function value for sheet 9.

S_NO	Icell	Vcell	Vest	Pref	Pest	AE	RE %	MBE
1	0.2046	21.5139	21.51968	4.401744	4.402926	0.005778	0.026857	2.23E-06
2	1.2619	19.6737	19.5779	24.82624	24.70535	0.095799	0.486939	0.000612
3	2.6433	18.7154	18.6624	49.47042	49.33032	0.053002	0.283201	0.000187
4	3.9734	17.9449	18.07571	71.30227	71.82203	0.130811	0.728958	0.001141
5	5.3206	17.5497	17.59286	93.37493	93.60455	0.043156	0.245907	0.000124
6	6.7019	17.1545	17.15542	114.9677	114.9739	0.000919	0.005359	5.63E-08
7	8.0491	16.6843	16.75861	134.2936	134.8917	0.07431	0.445386	0.000368
8	10.7265	15.8752	16.0031	170.2853	171.6573	0.127902	0.805673	0.001091
9	13.472	15.1411	15.212	203.9809	204.9361	0.070901	0.46827	0.000335
10	16.1494	14.4634	14.35228	233.5752	231.7807	0.111122	0.768295	0.000823
11	17.4795	14.087	13.85842	246.2337	242.2382	0.228581	1.622638	0.003483
12	18.8438	13.5792	13.26817	255.8837	250.0228	0.311027	2.290463	0.006449
13	20.1739	12.6772	12.54771	255.7486	253.1363	0.129485	1.021404	0.001118
14	21.5382	10.8743	11.47597	234.2128	247.1717	0.60167	5.532958	0.024134
15	22.9025	8.9213	8.794868	204.3201	201.4245	0.126432	1.417191	0.001066
						0.140726	1.076633	0.002729

Table 22. Performance metrics of AOAAO algorithm for sheet 9.

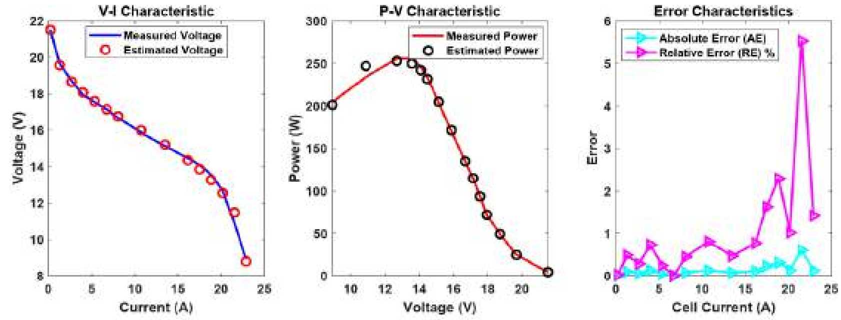

(a)

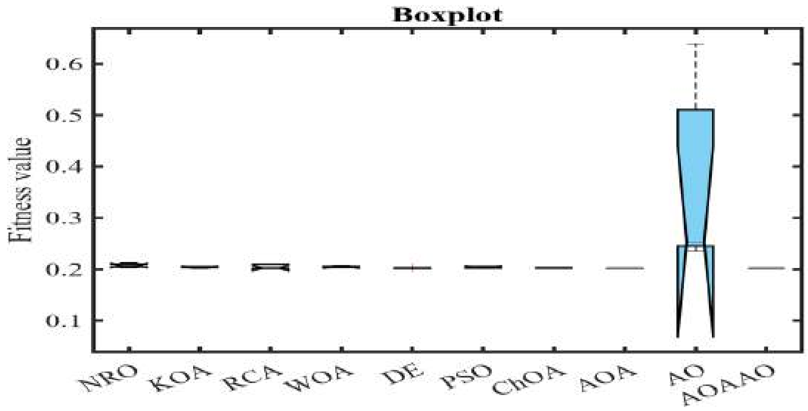

(b)

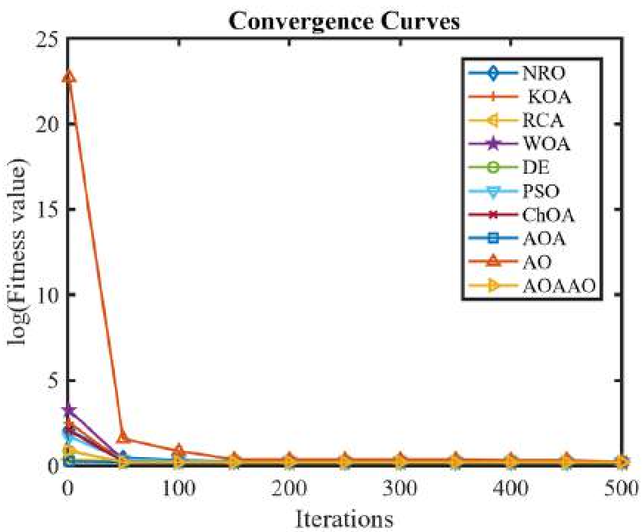

(c)

Fig. 11. AOAAO algorithm characteristic curves of Sheet 9; (**a**) V/I, P/V, and error curve, (**b**) Box-Plot, (**c**) convergence curve for Sheet 9.

Algorithm	NRO	KOA	RCA	WOA	DE	PSO	ChOA	AOA	AO	AOAAO
ξ_1	− 0.93693	− 0.87351	− 0.8532	− 1.17003	− 1.13816	− 1.13964	− 1.04212	− 0.88771	− 1.17864	− 0.88288
ξ_2	0.002781	0.002296	0.002068	0.003536	0.003356	0.003018	0.003221	0.002796	0.002993	0.002954
ξ_3	7.28E-05	4.92E-05	0.000036	8.01E-05	7.32E-05	4.69E-05	8.37E-05	8.47E-05	3.63E-05	9.79E-05
ξ_4	− 0.00014	− 0.00014	− 0.00014	− 0.00014	− 0.00014	− 0.00014	− 0.00014	− 0.00014	− 0.00014	− 0.00014
λ	14	14.00006	14	14	14.00446	14	14	14.00191	14.05939	14
R_c	0.0008	0.000761	0.0008	0.000613	0.000799	0.000765	0.0008	0.0008	0.000435	0.0008
B	0.015457	0.015628	0.0136	0.01606	0.01548	0.015438	0.015275	0.015418	0.017097	0.015503
Min.	0.104644	0.104672	0.111614	0.105873	0.104474	0.105137	0.104604	0.104475	0.110681	0.104446
Max.	0.124174	0.112918	0.111614	0.111339	0.105529	0.108858	0.10525	0.104525	0.361792	0.104446
Mean	0.111453	0.107917	0.111614	0.108099	0.104789	0.106378	0.104818	0.104493	0.183929	0.104446
Std.	0.007655	0.0043	7.85E-17	0.00231	0.000453	0.001505	0.000268	1.95E-05	0.102817	1.37E-16
RT	3.036326	3.035529	2.623905	2.789227	5.692173	3.393321	3.369347	3.993322	6.102912	0.113806
FR	7.8	5.8	8.4	6.6	3.4	5.8	4.2	2.4	9.6	1

Table 23. Optimized parameters and optimal function value for sheet 10.

S_NO	Icell	Vcell	Vest	Pref	Pest	AE	RE %	MBE
1	0.2729	23.541	23.47401	6.424339	6.406057	0.066992	0.284575	0.000299
2	1.279	21.4756	21.55584	27.46729	27.56992	0.080244	0.37365	0.000429
3	2.6603	20.3484	20.53214	54.13285	54.62166	0.183743	0.902983	0.002251
4	3.9734	19.8969	19.89719	79.05834	79.05949	0.00029	0.001457	5.6E-09
5	5.3547	19.4642	19.36757	104.225	103.7075	0.09663	0.496449	0.000622
6	6.719	19.0127	18.91714	127.7463	127.1043	0.09556	0.502611	0.000609
7	8.0321	18.5049	18.52373	148.6332	148.7845	0.018835	0.101782	2.36E-05
8	10.7265	17.8835	17.78336	191.8274	190.7532	0.100136	0.559937	0.000668
9	13.472	17.2808	17.06738	232.8069	229.9317	0.213425	1.235039	0.003037
10	16.1664	16.2089	16.3588	262.0396	264.4628	0.149896	0.924778	0.001498
11	17.4966	15.8701	15.99328	277.6728	279.8281	0.123182	0.77619	0.001012
12	18.8608	15.5312	15.59617	292.9309	294.1562	0.064966	0.418293	0.000281
13	20.191	15.1923	15.17005	306.7477	306.2985	0.022249	0.146447	3.3E-05
14	21.5553	14.6282	14.64549	315.3152	315.6879	0.01729	0.118199	1.99E-05
15	22.9195	13.745	13.70155	315.0285	314.0326	0.043454	0.316147	0.000126
						0.085126	0.477236	0.000727

Table 24. Performance metrics of AOAAO algorithm for sheet 10.

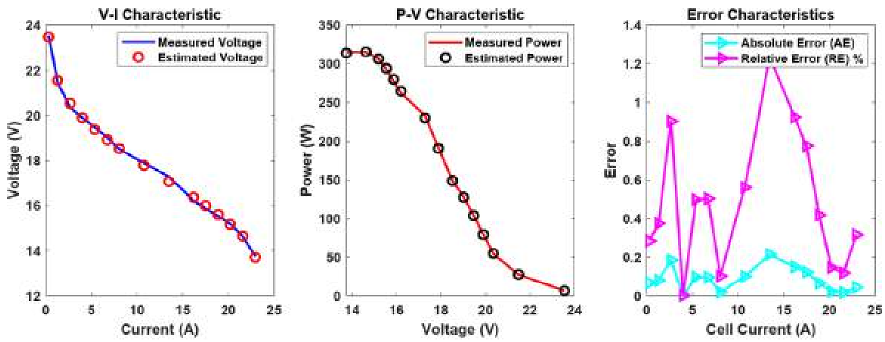

(a)

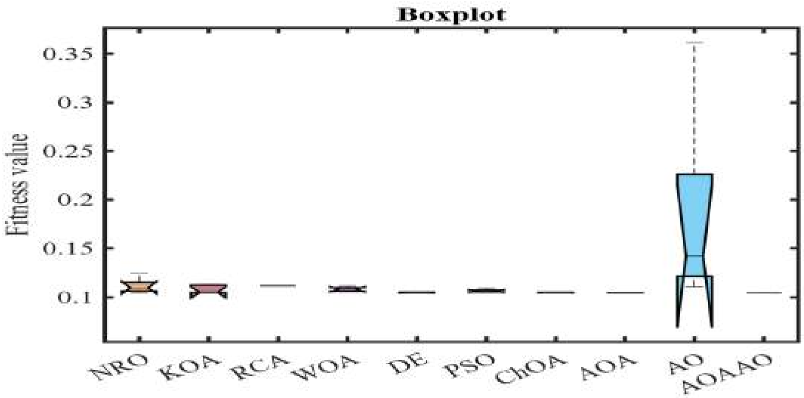

(b)

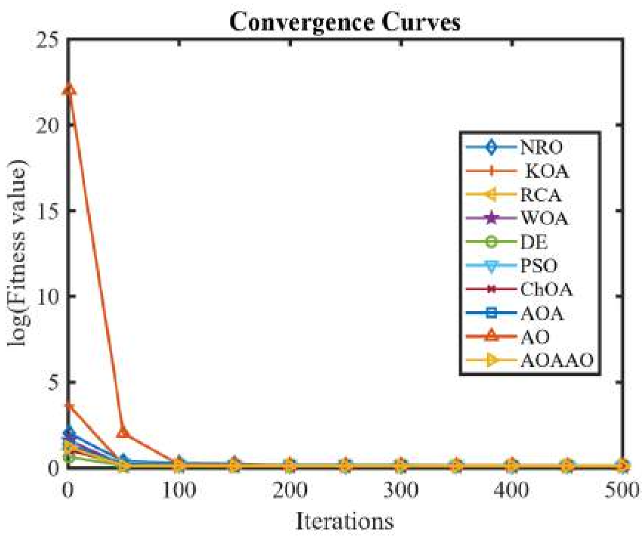

(c)

Fig. 12. AOAAO algorithm characteristic curves of Sheet 10; (**a**) V/I, P/V, and error curve, (**b**) box-plot, (**c**) convergence curve for Sheet 10.

Algorithm	NRO	KOA	RCA	WOA	DE	PSO	ChOA	AOA	AO	AOAAO
ξ_1	− 0.88459	− 0.9085	− 0.8532	− 0.862	− 1.15201	− 1.19969	− 0.9855	− 1.1026	− 0.94137	− 0.85321
ξ_2	0.002528	0.001751	0.002204	0.002431	0.002897	0.002917	0.002813	0.002442	0.001938	0.001626
ξ_3	9.8E-05	0.000036	8.2E-05	9.64E-05	6.06E-05	5.06E-05	9.44E-05	3.95E-05	4.38E-05	4.03E-05
ξ_4	− 9.5E-05	− 9.5E-05	− 9.5E-05	− 9.5E-05	− 9.5E-05	− 9.5E-05	− 9.5E-05	− 9.5E-05	− 0.00011	− 9.5E-05
λ	23	23	23	22.39673	22.99999	23	23	22.99564	23	23
R_c	0.0001	0.0001	0.0001	0.000132	0.0001	0.0008	0.0001	0.000101	0.00031	0.0001
B	0.034892	0.034809	0.034812	0.034858	0.03481	0.033887	0.034765	0.034829	0.023682	0.034812
Min.	0.075486	0.075484	0.075484	0.075532	0.075484	0.075794	0.075485	0.075485	0.094086	0.075484
Max.	0.083937	0.075626	0.076392	0.075845	0.075906	0.076236	0.075518	0.075489	0.130321	0.076103
Mean	0.078049	0.075552	0.075774	0.075676	0.075598	0.075988	0.075492	0.075487	0.109496	0.075608
Std.	0.003401	5.18E-05	0.000371	0.000127	0.000181	0.000159	1.45E-05	1.68E-06	0.015258	0.000277
RT	3.01885	2.984287	2.584432	2.679743	5.528724	3.123379	3.306627	3.865363	6.019614	0.120014
FR	8	4.4	5	6.2	4.6	7.8	3.2	3.4	10	2.4

Table 25. Optimized parameters and optimal function value for sheet 11.

S_NO	Icell	Vcell	Vest	Pref	Pest	AE	RE %	MBE
1	0.104	9.53	9.707991	0.99112	1.009631	0.177991	1.867695	0.002112
2	0.199	9.38	9.438401	1.86662	1.878242	0.058401	0.62261	0.000227
3	0.307	9.2	9.244289	2.8244	2.837997	0.044289	0.481397	0.000131
4	0.403	9.24	9.112618	3.72372	3.672385	0.127382	1.378594	0.001082
5	0.511	9.1	8.988223	4.6501	4.592982	0.111777	1.228322	0.000833
6	0.614	8.94	8.883388	5.48916	5.4544	0.056612	0.63324	0.000214
7	0.704	8.84	8.798598	6.22336	6.194213	0.041402	0.468344	0.000114
8	0.806	8.75	8.707211	7.0525	7.018012	0.042789	0.48902	0.000122
9	0.908	8.66	8.618539	7.86328	7.825634	0.041461	0.478761	0.000115
10	1.075	8.45	8.474217	9.08375	9.109783	0.024217	0.28659	3.91E-05
11	1.126	8.41	8.429356	9.46966	9.491455	0.019356	0.23016	2.5E-05
12	1.28	8.2	8.28806	10.496	10.60872	0.08806	1.073907	0.000517
13	1.39	8.14	8.178149	11.3146	11.36763	0.038149	0.468666	9.7E-05
14	1.45	8.11	8.11327	11.7595	11.76424	0.00327	0.040322	7.13E-07
15	1.57	8	7.967689	12.56	12.50927	0.032311	0.403891	6.96E-05
						0.060498	0.676768	0.00038

Table 26. Performance metrics of AOAAO algorithm for sheet 11.

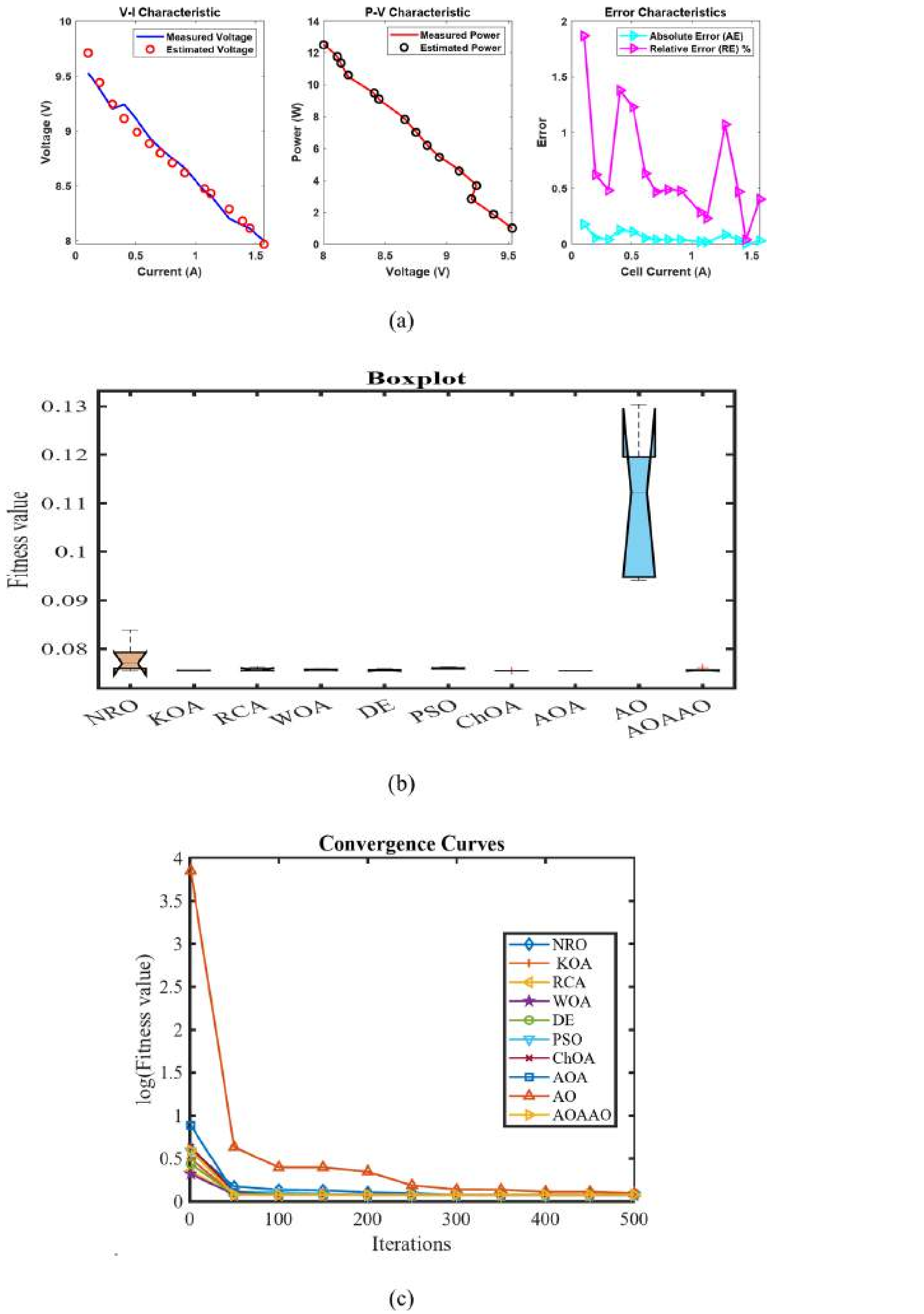

Fig. 13. AOAAO algorithm characteristic curves of Sheet 11; (**a**) V/I, P/V, and error curve, (**b**) Box-Plot, (**c**) convergence curve for Sheet 11.

Algorithm	NRO	KOA	RCA	WOA	DE	PSO	ChOA	AOA	AO	AOAAO
ξ_1	− 1.02678	− 1.02507	− 0.8532	− 1.15414	− 1.06547	− 0.9719	− 0.94436	− 0.94005	− 1.15869	− 0.8532
ξ_2	0.002472	0.002259	0.001615	0.002966	0.002638	0.002236	0.002364	0.002476	0.002595	0.001615
ξ_3	5.77E-05	4.27E-05	0.000036	6.39E-05	6.07E-05	5.34E-05	6.89E-05	7.8E-05	3.68E-05	3.6E-05
ξ_4	− 9.5E-05	− 9.5E-05	− 9.5E-05	− 9.5E-05	− 9.5E-05	− 9.5E-05	− 9.5E-05	− 9.5E-05	− 9.9E-05	− 9.5E-05
λ	21.80783	14.00637	14	15.11864	14.08594	14.35789	14	14.00895	15.16289	14
R_c	0.0001	0.00079	0.0008	0.000136	0.000465	0.00014	0.0008	0.000598	0.000704	0.0008
B	0.050921	0.048497	0.048483	0.04963	0.048921	0.049301	0.048488	0.048723	0.044511	0.048483
Min.	0.064291	0.064194	0.064194	0.064212	0.0642	0.064208	0.064194	0.064196	0.067024	0.064194
Max.	0.087937	0.064255	0.064237	0.064231	0.064233	0.064255	0.064199	0.064225	0.114381	0.064194
Mean	0.075448	0.064208	0.064211	0.06422	0.064216	0.064227	0.064196	0.064206	0.092923	0.064194
Std.	0.010334	2.64E-05	2.4E-05	7.2E-06	1.35E-05	1.71E-05	1.84E-06	1.15E-05	0.021361	1.31E-16
RT	2.991223	3.038752	2.577866	2.704654	5.503941	3.083598	3.35498	3.799408	5.996674	0.129202
FR	9.2	4.2	4	6	6.2	6.6	3.6	4.2	9.8	1.2

Table 27. Optimized parameters and optimal function value for sheet 12.

S_NO	Icell	Vcell	Vest	Pref	Pest	AE	RE %	MBE
1	0.097	9.87	9.999676	0.95739	0.969969	0.129676	1.313835	0.001121
2	0.115	9.84	9.926757	1.1316	1.141577	0.086757	0.881673	0.000502
3	0.165	9.77	9.767163	1.61205	1.611582	0.002837	0.02904	5.37E-07
4	0.204	9.7	9.669211	1.9788	1.972519	0.030789	0.317416	6.32E-05
5	0.249	9.61	9.573412	2.39289	2.38378	0.036588	0.380725	8.92E-05
6	0.273	9.59	9.527679	2.61807	2.601056	0.062321	0.649859	0.000259
7	0.326	9.5	9.436217	3.097	3.076207	0.063783	0.671399	0.000271
8	0.396	9.4	9.329837	3.7224	3.694616	0.070163	0.746413	0.000328
9	0.5	9.26	9.191099	4.63	4.595549	0.068901	0.744073	0.000316
10	0.621	9.05	9.046907	5.62005	5.618129	0.003093	0.034173	6.38E-07
11	0.711	8.93	8.946522	6.34923	6.360977	0.016522	0.185017	1.82E-05
12	0.797	8.83	8.853561	7.03751	7.056288	0.023561	0.266829	3.7E-05
13	1.006	8.54	8.63028	8.59124	8.682062	0.09028	1.057145	0.000543
14	1.141	8.42	8.481146	9.60722	9.676988	0.061146	0.726203	0.000249
15	1.37	8.27	8.200534	11.3299	11.23473	0.069466	0.839981	0.000322
						0.054392	0.589585	0.000275

Table 28. Performance metrics of AOAAO algorithm for sheet 12.

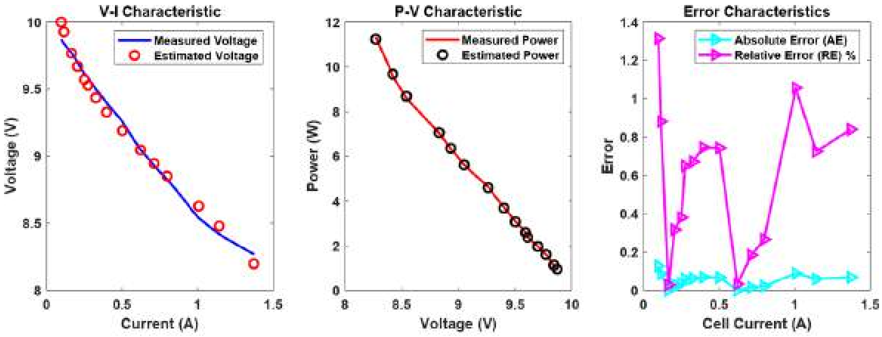

(a)

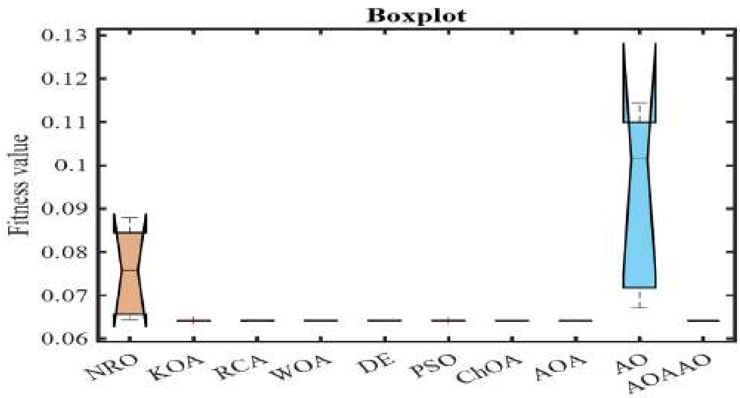

(b)

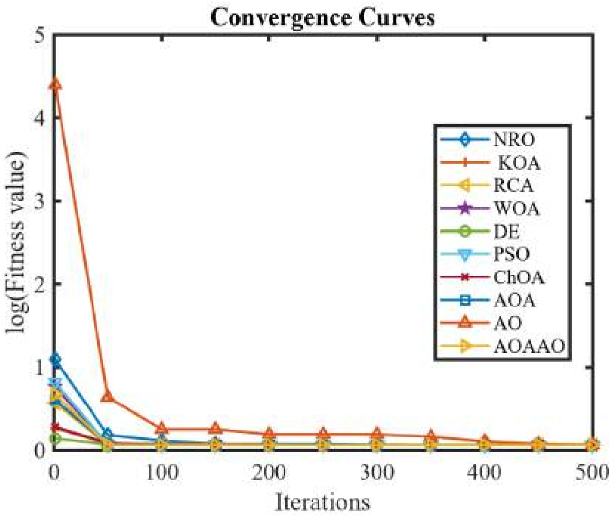

(c)

Fig. 14. AOAAO algorithm characteristic curves of Sheet 12; (**a**) V/I, P/V, and error curve, (**b**) box-plot, (**c**) convergence curve for Sheet 12.

Data availability

The data presented in this study are available through email upon request to the corresponding author.

Received: 11 December 2024; Accepted: 6 February 2025
Published online: 11 February 2025

References

1. Mutezo, G. & Mulopo, J. A review of Africa's transition from fossil fuels to renewable energy using circular economy principles. *Renew. Sustain. Energy Rev.* **137**, 110609 (2021).
2. Obileke, K., Onyeaka, H., Meyer, E. L. & Nwokolo, N. Microbial fuel cells, a renewable energy technology for bio-electricity generation: a mini-review. *Electrochem. Commun.* **125**, 107003 (2021).
3. Abdelkareem, M. A. et al. Environmental aspects of fuel cells: a review. *Sci. Total Environ.* **752**, 141803 (2021).
4. Huang, Z., Xing, L. & Tu, Z. Load changing characteristics of the hydrogen-air and hydrogen-oxygen proton exchange membrane fuel cells. *Int. J. Energy Res.* **46** (2), 1909–1921 (2022).
5. Meng, K. et al. Investigation on degradation mechanism of hydrogen–oxygen proton exchange membrane fuel cell under current cyclic loading. *Energy* **242**, 123045 (2022).
6. Çalışır, D., Ekici, S., Midilli, A. & Karakoc, T. H. Benchmarking environmental impacts of power groups used in a designed UAV: hybrid hydrogen fuel cell system versus lithium-polymer battery drive system. *Energy* **262**, 125543 (2023).
7. Qu, E. et al. Proton exchange membranes for high temperature proton exchange membrane fuel cells: challenges and perspectives. *J. Power Sources*. **533**, 231386 (2022).
8. Xu, Q. et al. A comprehensive review of solid oxide fuel cells operating on various promising alternative fuels. *Energy. Conv. Manag.* **253**, 115175 (2022).
9. Samanta, S. & Roy, D. Molten carbonate fuel cell integrated hybrid system for clean and efficient power generation. *Appl. Therm. Eng.* **226**, 120294 (2023).
10. Corigliano, O., Pagnotta, L. & Fragiacomo, P. On the technology of solid oxide fuel cell (SOFC) energy systems for stationary power generation: a review. *Sustainability* **14** (22), 15276 (2022).
11. Jadhav, D. A. et al. Current outlook towards feasibility and sustainability of ceramic membranes for practical scalable applications of microbial fuel cells. *Renew. Sustain. Energy Rev.* **167**, 112769 (2022).
12. Elkafas, A. G., Rivarolo, M., Gadducci, E., Magistri, L. & Massardo, A. F. Fuel cell systems for maritime: a review of research development, commercial products, applications, and perspectives. *Processes* **11** (1), 97 (2022).
13. Chen, X. et al. Performance evaluation on thermodynamics-economy-environment of PEMFC vehicle power system under dynamic condition. *Energy. Conv. Manag.* **269**, 116082 (2022).
14. Fan, L., Tu, Z. & Chan, S. H. Recent development of hydrogen and fuel cell technologies: a review. *Energy Rep.* **7**, 8421–8446 (2021).
15. Aminudin, M. A. et al. An overview: current progress on hydrogen fuel cell vehicles. *Int. J. Hydrog. Energy*. **48** (11), 4371–4388 (2023).
16. Hussien, A. M., Hasanien, H. M. & Mekhamer, S. F. Sunflower optimization algorithm-based optimal PI control for enhancing the performance of an autonomous operation of a microgrid. *Ain Shams Eng. J.* **12** (2), 1883–1893 (2021).
17. Meng, K., Chen, B., Zhou, H., Shen, J. & Tu, Z. Experimental investigation on voltage response characteristics of hydrogen-oxygen proton exchange membrane fuel cells under gas starvation. *Energy. Conv. Manag.* **268**, 115973 (2022).
18. Korkmaz, S. A. et al. Comparison of various metaheuristic algorithms to extract the optimal PEMFC modeling parameters. *Int. J. Hydrog. Energy*. **51**, 1402–1420 (2024).
19. Kanouni, B. & Mekhilef, S. A multi-objective model predictive current control with two-step horizon for double-stage grid-connected inverter PEMFC system. *Int. J. Hydrog. Energy*. **47** (4), 2685–2707 (2022).
20. Zhao, X. et al. Classification, summarization and perspective on modeling techniques for polymer electrolyte membrane fuel cell. *Int. J. Hydrog. Energy*. **48** (57), 21864–21885 (2023).
21. Hussien, A. M. et al. Coot bird algorithms-based tuning PI controller for optimal microgrid autonomous operation. *IEEE Access.* **10**, 6442–6458 (2022).
22. Chen, Y., Pi, D., Wang, B., Chen, J. & Xu, Y. Bi-subgroup optimization algorithm for parameter estimation of a PEMFC model. *Expert Syst. Appl.* **196**, 116646 (2022).
23. Ashraf, H., Abdellatif, S. O., Elkholy, M. M. & ElFergany, A. A. Computational techniques based on artificial intelligence for extracting optimal parameters of PEMFCs: Survey and insights. *Arch. Comput. Methods Eng.* **29** (6), 3943–3972 (2022).
24. Mitra, U., Arya, A. & Gupta, S. A comprehensive and comparative review on parameter estimation methods for modelling proton exchange membrane fuel cell. *Fuel* **335**, 127080 (2023).
25. Ćalasan, M., Micev, M., Hasanien, H. M. & Aleem, S. H. A. PEM fuel cells: two novel approaches for mathematical modeling and parameter estimation. *Energy* **290**, 130130 (2024).
26. Zhou, H. et al. Model optimization of a high-power commercial PEMFC system via an improved grey wolf optimization method. *Fuel* **357**, 129589 (2024).
27. Zhao, Y., Luo, M., Yang, J., Chen, B. & Sui, P. C. Numerical analysis of PEMFC stack performance degradation using an empirical approach. *Int. J. Hydrog. Energy*. **56**, 147–163 (2024).
28. Diab, A. A. Z. & Abdelhamid, A. M. Optimal identification of model parameters for PEMFCs using neoteric metaheuristic methods. *IET Renew. Power Gener.* **17** (3), 659–680 (2023).
29. Sultan, H. M., Menesy, A. S., Alqahtani, M., Khalid, M. & Diab, A. A. Z. Accurate parameter identification of proton exchange membrane fuel cell models using different metaheuristic optimization algorithms. *Energy Rep.* **10**, 4824–4848 (2023).
30. Liu, X. et al. Uncertainty assessment of a semi-empirical output voltage model for proton exchange membrane fuel cells. *Int. J. Hydrog. Energy*. **48** (29), 11071–11085 (2023).
31. Wang, Y. et al. Degradation prediction of proton exchange membrane fuel cell stack using semi-empirical and data-driven methods. *Energy AI*. **11**, 100205 (2023).
32. Abbou, A., El Hasnaoui, A., Khan, S. S. & Yamin, F. Analysis of the novel dynamic semiempirical model of proton exchange membrane fuel cell by incorporating ambient condition variations. *Int. J. Energy Environ. Eng.* **13** (1), 105–120 (2022).
33. Yuan, K., Ma, Y., Zhang, H., Razmjooy, N. & Ghadimi, N. Optimal parameters estimation of the proton exchange membrane fuel cell stacks using a combined owl search algorithm. *Energy Sources Part. Recovery Utilization Environ. Eff.* **45** (4), 11712–11732 (2023).
34. Abbassi, R. et al. Accurate key parameters estimation of PEMFCs' models based on dandelion optimization algorithm. *Mathematics* **11** (6), 1298 (2023).
35. Kaur, S., Awasthi, L. K., Sangal, A. L. & Dhiman, G. Tunicate Swarm Algorithm: a new bio-inspired based metaheuristic paradigm for global optimization. *Eng. Appl. Artif. Intell.* **90**, 103541 (2020).
36. Abualigah, L. et al. Aquila optimizer: a novel meta-heuristic optimization algorithm. *Comput. Ind. Eng.* **157**, 107250 (2021).
37. Wei, Z., Huang, C., Wang, X., Han, T. & Li, Y. Nuclear reaction optimization: a novel and powerful physics-based algorithm for global optimization. *IEEE Access.* **7**, 66084–66109 (2019).
38. Abdel-Basset, M., Mohamed, R., Azeem, S. A. A., Jameel, M. & Abouhawwash, M. Kepler optimization algorithm: a new metaheuristic algorithm inspired by Kepler's laws of planetary motion. *Knowl. Based Syst.* **268**, 110454 (2023).
39. Hassan, D. S., Fahmy, H. M. & Bahaa-ElDin, A. M. RCA: efficient connected dominated clustering algorithm for mobile ad hoc networks. *Comput. Netw.* **75**, 177–191 (2014).
40. Mirjalili, S. & Lewis, A. The whale optimization algorithm. *Adv. Eng. Softw.* **95**, 51–67 (2016).
41. Karaboğa, D. & Ökdem, S. A simple and global optimization algorithm for engineering problems: differential evolution algorithm. *Turkish J. Electr. Eng. Comput. Sci.* **12** (1), 53–60 (2004).
42. Wang, D., Tan, D. & Liu, L. Particle swarm optimization algorithm: an overview. *Soft. Comput.* **22** (2), 387–408 (2018).

43. Saffari, A., Khishe, M. & Zahiri, S. H. Fuzzy-ChOA: an improved chimp optimization algorithm for marine mammal classification using artificial neural network. *Analog Integr. Circuits Signal Process.* **111** (3), 403–417 (2022).
44. Abualigah, L., Diabat, A., Mirjalili, S., Abd Elaziz, M. & Gandomi, A. H. The arithmetic optimization algorithm. *Comput. Methods Appl. Mech. Eng.* **376**, 113609 (2021).
45. Sultan, H. M., Menesy, A. S., Hassan, M. S., Jurado, F. & Kamel, S. Standard and quasi oppositional bonobo optimizers for parameter extraction of PEM fuel cell stacks. *Fuel* **340**, 127586 (2023).
46. Chen, Y. & Zhang, G. New parameters identification of Proton exchange membrane fuel cell stacks based on an improved version of African vulture optimization algorithm. *Energy Rep.* **8**, 3030–3040 (2022).
47. Menesy, A. S., Sultan, H. M., Selim, A., Ashmawy, M. G. & Kamel, S. Developing and applying chaotic harris hawks optimization technique for extracting parameters of several proton exchange membrane fuel cell stacks. *IEEE Access.* **8**, 1146–1159 (2019).
48. Chen, J. H. et al. Modeling and temperature control of a water-cooled PEMFC system using intelligent algorithms. *Appl. Energy*. **372**, 123790–123790 (2024).
49. Babay, M. A. et al. Comparative sustainability analysis of serpentine flow-field and straight channel PEM fuel cell designs. *Int. J. Syst. Assur. Eng. Manage.* **15** (8), 3954–3970 (2024).
50. Babay, M. A. et al. Numerical simulation and thermal analysis of pressurized hydrogen vehicle cylinders: impact of geometry and phase change materials. *J. Adv. Res. Fluid Mech. Therm. Sci.* **117** (2), 71–90 (2024).
51. Babay, M. A. et al. Integrated thermodynamic analysis and channel variation effects on solid oxide electrolysis for efficient hydrogen generation. *Procedia Comput. Sci.* **236**, 152–159 (2024).
52. Babay, M. A., Adar, M., Chebak, A. & Mabrouki, M. Forecasting green hydrogen production: an assessment of renewable energy systems using deep learning and statistical methods. *Fuel* **381**, 133496–133496 (2024).
53. Babay, M-A. et al. Exploring the sustainability of serpentine flow-field fuel cell, straight channel PEM fuel cells hight temperature through numerical analysis. *Energy Nexus*. **1**, 100283–100283 (2024).
54. Waseem, M., Amir, M., Lakshmi, G. S., Harivardhagini, S. & Ahmad, M. Fuel cell-based hybrid electric vehicles: an integrated review of current status, key challenges, recommended policies, and future prospects. *Green. Energy Intell. Transp.* **2** (6), 100121 (2023).
55. Gao, Y. & Lin, M. Research on the performance characteristics of hydrogen circulation pumps for PEMFC vehicles. *Int. J. Hydrog. Energy*. **50**, 1255–1272 (2023).
56. Qiu, Y. et al. Progress and challenges in multi-stack fuel cell system for high power applications: architecture and energy management. *Green. Energy Intell. Transp.* **2** (2), 100068 (2023).
57. Wan, W. et al. Operating conditions combination analysis method of optimal water management state for PEM fuel cell. *Green. Energy Intell. Transp.* **2** (4), 100105–100105 (2023).
58. Rosli, M. I. et al. Performance analysis of PEMFC with single-channel and multi-channels on the impact of the geometrical model. *Energies* **15** (21), 7960 (2022).
59. Zhang, Y., Huang, C., Huang, H. & Wu, J. Multiple learning neural network algorithm for parameter estimation of proton exchange membrane fuel cell models. *Green. Energy Intell. Transp.* **1**, 100040 (2022).
60. Abdel-Basset, M., Mohamed, R., Elhoseny, M., Chakrabortty, R. K. & Ryan, M. J. An efficient heap-based optimization algorithm for parameters identification of proton exchange membrane fuel cells model: analysis and case studies. *Int. J. Hydrog. Energy*. **46** (21), 11908–11925 (2021).
61. Kandidayeni, M. et al. Benchmark of proton exchange membrane fuel cell parameters extraction with metaheuristic optimization algorithms. *Energy* **183**, 912–925 (2019).
62. Rosli, R. E. et al. The design and development of an HT-PEMFC test cell and test station. *Int. J. Hydrog. Energy*. **44** (58), 30763–30771 (2019).
63. Abd Rahman, S. N. et al. Simulation of PEMFC stack for portable power generator application. *Jurnal Kejuruteraan*. **1** (1), 1 (2018).
64. Yusuf, N. Y., Masdar, M. S., Isahak, W. N. R. W., Nordin, D. & Husaini, T. Challenges and prospects of bio-hydrogen production for PEMFC application: a review. *Int. J. Appl. Eng. Res.* **11** (19), 9960–9969 (2016).
65. Lim, B. H., Majlan, E. H., Daud, W. R. W., Husaini, T. & Rosli, M. I. Effects of flow field design on water management and reactant distribution in PEMFC: a review. *Ionics* **22**, 301–316 (2016).
66. Cheng, S. J., Miao, J. M. & Wu, S. J. Use of metamodeling optimal approach promotes the performance of proton exchange membrane fuel cell (PEMFC). *Appl. Energy*. **105**, 161–169 (2013).

Acknowledgements
The authors would like to acknowledge the funding from the Ministry of Higher Education Malaysia, through a Fundamental Research Grant Scheme (FRGS) with code FRGS/1/2023/TK08/UKM/02/5. The authors would also like to acknowledge the support of the Centre for research and Instrumentation Management, UKM, for the testing equipment.

Author contributions
M.K.S., M.A.S.A., and R.K. conceptualized the study and developed the methodology. M.K.S. and P.J. performed the experimental work and data collection. M.K., G.G., and H.A.M. contributed to the computational modeling and algorithm design. R.K. and M.K. performed the data analysis and interpretation. M.K.S. and M.K. prepared the manuscript draft. G.G. and H.A.M. critically reviewed and revised the manuscript for important intellectual content. All authors contributed to the writing process, provided feedback, and approved the final manuscript for publication.

Declarations

Competing interests
The authors declare no competing interests.

Additional information
Correspondence and requests for materials should be addressed to M.K.S., M.K. or G.G.